bioRxiv preprint doi: https://doi.org/10.1101/470054; this version posted November 18, 2018. The copyright holder for this preprint (which was not certified by peer review) is the author/funder, who has granted bioRxiv a license to display the preprint in perpetuity. It is made available under aCC-BY-NC-ND 4.0 International license.

High inter- and intraspecific turnover of satellite repeats in great apes

Monika Cechova

Department of Biology, Pennsylvania State University, University Park, PA 16802 USA

biomonika@psu.edu

Robert S. Harris

Department of Biology, Pennsylvania State University, University Park, PA 16802 USA

rsharris@bx.psu.edu

Marta Tomaszkiewicz

Department of Biology, Pennsylvania State University, University Park, PA 16802 USA

mat19@psu.edu

Barbara Arbeithuber

Department of Biology, Pennsylvania State University, University Park, PA 16802 USA

bxa15@psu.edu

Francesca Chiaromonte

Department of Biology, Pennsylvania State University, University Park, PA 16802 USA

Department of Statistics, Pennsylvania State University, University Park, PA 16802 USA

EMbeDS, Sant'Anna School of Advanced Studies, Pisa, 56127 Italy

Center for Medical Genomics, Penn State, University Park, PA 16802 USA

fxc11@psu.edu, co-corresponding author

Kateryna D. Makova

Department of Biology, Pennsylvania State University, University Park, PA 16802 USA

Center for Medical Genomics, Penn State, University Park, PA 16802 USA

kdm16@psu.edu, co-corresponding author

bioRxiv preprint doi: https://doi.org/10.1101/470054; this version posted November 18, 2018. The copyright holder for this preprint (which was not certified by peer review) is the author/funder, who has granted bioRxiv a license to display the preprint in perpetuity. It is made available under aCC-BY-NC-ND 4.0 International license.

Abstract

Background. Satellite repeats are a structural component of centromeres and telomeres, and in some instances their divergence is known to drive speciation. Due to their highly repetitive nature, satellite sequences have been understudied and underrepresented in genome assemblies. To investigate their turnover in great apes, we studied satellite repeats in human, chimpanzee, bonobo, gorilla, and Sumatran and Bornean orangutans, using unassembled short and long sequencing reads.

Results. The density of satellite repeats, as identified from accurate short reads (Illumina), varied greatly among great ape genomes. These were dominated by a handful of abundant repeated motifs, frequently shared among species, which formed two groups: (1) the $(AATGG)_n$ repeat (critical for heat shock response) and its derivatives; and (2) subtelomeric 32-mers. Using the densities of abundant repeats, individuals could be classified into species. However clustering did not reproduce the accepted species phylogeny, suggesting rapid repeat evolution. Several abundant repeats were enriched in males vs. females; using existing Y chromosome assemblies or FIuorescent In Situ Hybridization, we validated location for some of them on the Y. Finally, applying a novel computational tool, we identified many satellite repeats completely embedded within long Oxford Nanopore and Pacific Biosciences reads. Such repeats were up to 59 kb in length and consisted of perfect repeats interspersed with other similar sequences.

Conclusions. Our results based on sequencing reads generated with three different technologies provide the first detailed characterization of great ape satellite repeats, and open new avenues for exploring their functions.

Keywords

heterochromatin, satellite, repeats, great apes, long reads

bioRxiv preprint doi: https://doi.org/10.1101/470054; this version posted November 18, 2018. The copyright holder for this preprint (which was not certified by peer review) is the author/funder, who has granted bioRxiv a license to display the preprint in perpetuity. It is made available under aCC-BY-NC-ND 4.0 International license.

Background

Heterochromatin and euchromatin were first described based on an observation of their contrasting compaction in chromosomes at the interphase; while *heterochromatin* is highly compacted, *euchromatin* is open (Heitz 1928). It was later found that, in contrast to euchromatin, heterochromatin is gene-poor and rarely transcribed. The regions of chromosomes that remain condensed throughout the cell cycle are comprised of *constitutive heterochromatin*, whereas the regions that undergo heterochromatization in response to cellular signals and gene activity are comprised of *facultative heterochromatin*. Heterochromatin is typically dominated by *satellite repeats* – long arrays of tandemly repeated non-coding DNA (Sueoka 1961; Kit 1961) that consist of smaller units organized into higher-order repeat structures, as observed, for instance, in alpha satellites at human centromeres (Sujiwattanarat et al. 2015). A similar enrichment of heterochromatin with satellite repeats is widespread at the centromeres of many animal and plant genomes (Melters et al. 2013).

While labeled as "junk DNA" in the past, it is now evident that heterochromatin fulfills important functions in the genome (Walker 1971; Yunis and Yasmineh 1971; Ferree and Barbash 2009). Centromeric heterochromatin ensures the correct segregation of sister chromatids in mitosis and meiosis. Satellite repeat expansions have been associated with changes in gene expression and methylation (Brahmachary et al. 2014; Quilez et al. 2016). It has also been proposed that heterochromatin aids in maintaining cellular identity by repressing genes that are not specific to a particular cell lineage (reviewed in (Becker, Nicetto, and Zaret 2016)). For instance, the heterochromatin-associated histone mark H3K9me3 blocks reprogramming to pluripotency (Soufi, Donahue, and Zaret 2012). Additionally, heterochromatin loss is part of the normal aging process (Zhang et al. 2015). Similarly, heterochromatin changes during stress. For instance, gene silencing at constitutive heterochromatin is less effective at high temperatures in yeast (Ayoub, Goldshmidt, and Cohen 1999; Gowen and Gay 1933); heterochromatin-induced gene inactivation (known as "position-effect variegation") is sensitive to temperature in both yeast and *Drosophila* (Allshire et al. 1995; Gowen and Gay 1933; Spofford 1976); and the latter effect was shown to be variable within a natural *Drosophila* population (Kelsey and Clark 2017). Moreover, in the rods of the retinas of nocturnal mammals, heterochromatin is localized towards the central regions of the nucleus and acts as a lens to channel light (Solovei et al. 2009).

Despite a growing interest in shedding light onto these important functions of heterochromatin, satellite repeats are frequently underrepresented in genomic studies – due to the difficulties in sequencing and assembling these highly similar sequences (Chaisson et al. 2015). Thus, and critically, they remain understudied. The lack of information about satellite repeats is particularly alarming given their high abundance, e.g., alpha satellites were estimated to constitute approximately 3% of the human genome (Manuelidis 1978; Hayden et al. 2013). Relatedly, satellite repeats are likely plentiful in yet unassembled gaps in the human genome (Miga et al. 2014; Stephens and Iyer 2018). One of the largest

bioRxiv preprint doi: https://doi.org/10.1101/470054; this version posted November 18, 2018. The copyright holder for this preprint (which was not certified by peer review) is the author/funder, who has granted bioRxiv a license to display the preprint in perpetuity. It is made available under aCC-BY-NC-ND 4.0 International license.

uncharacterized gaps in the human genome is located in the Male-Specific region of the Y chromosome (MSY), which contains six types of satellite repeat sequences (DYZ1, DYZ2, DYZ3, DYZ17, DYZ18, and DYZ19) (Skaletsky et al. 2003).

Heterochromatin exhibits remarkable *interspecific* variability in size and structure. Such variability can be frequently observed even between closely related species. For instance, on the long arm of the Y chromosome, heterochromatin is the major component in human and gorilla, but is virtually absent in chimpanzee (Gläser et al. 1998) — notwithstanding the fact that human, gorilla, and chimpanzee diverged less than 8 million years (MY) ago (Glazko & Nei, 2003). As another example, whereas 20% of the genome of *Drosophila melanogaster* is composed of satellite DNA, this percentage is as low as 0.5% for *D. erecta* and as high as 50% for *D. virilis (Gall, Cohen, and Polan 1971; Lohe and Brutlag 1987)*; divergence times are estimated at 13 MY between *D. erecta* and *D. melanogaster*, and at 63 MY between *D. virilis* and *D. melanogaster* (Tamura, Subramanian, and Kumar 2004). The differences in satellite repeat abundance in nine *Drosophila* species were proposed to result predominantly from lineage-specific gains accumulated over the past 40 MY of evolution (Wei et al. 2018). Due to its rapid evolutionary turnover, heterochromatin can serve as a species barrier (Yunis and Yasmineh 1971). For instance, the female hybrids between *D. melanogaster* males and *D. simulans* females are not viable because, during cell division, they fail to properly separate the satellite 359-bp repeat on the X chromosome (Ferree and Barbash 2009; Rošić, Köhler, and Erhardt 2014).

Profound *intraspecific* variability in heterochromatin has also been reported, including that among humans (Altemose et al. 2014; Miga et al. 2014). For instance, the length of the DYZ1 satellite repeat varies considerably among major Y chromosome haplogroups; DYZ1 is longer in Y chromosomes belonging to the predominantly Asian O haplogroup than in those belonging to the predominantly African E haplogroup (Altemose et al. 2014). The centromeric array of the X chromosome was shown to vary in length among different human populations by as much as an order of magnitude (0.5-5 Mb) (Miga et al. 2014). Some human neocentromeres were found to harbor only very short (as short as 15-kb) heterochromatin domains leading to a defect in sister chromatid cohesion (Alonso et al. 2010).

In this study, we characterize satellite repeat turnover among six great ape species – human, chimpanzee, bonobo, gorilla, Bornean orangutan, and Sumatran orangutan – which diverged less than ~14 MY ago (Goodman, Grossman, and Wildman 2005). We focus on repeats that constitute portions of long arrays of satellite DNA and use them as a proxy for heterochromatin (Wei et al. 2014). This approximation is needed because of challenges in the direct identification of heterochromatin due to its transient nature in various cells of an individual throughout their lifetime. In this manuscript, we, first, identify satellite repeats in short sequencing reads generated with the low-error-rate Illumina technology, and investigate their inter- and intraspecific variation. We pinpoint repeats with higher incidence in males than females and, for some of these repeats, confirm location on the Y chromosome using existing Y

bioRxiv preprint doi: https://doi.org/10.1101/470054; this version posted November 18, 2018. The copyright holder for this preprint (which was not certified by peer review) is the author/funder, who has granted bioRxiv a license to display the preprint in perpetuity. It is made available under aCC-BY-NC-ND 4.0 International license.

assemblies or fluorescent in situ hybridization (FISH). Next, by analyzing human trio data, we investigate how satellite repeat densities change from generation to generation. Lastly, we use the repeated motifs identified from low-error-rate short reads as queries to decipher the lengths and densities of ape satellite repeats from error-prone long reads (both Pacific Biosciences, or PacBio, and Oxford Nanopore, or Nanopore). To the best of our knowledge, ours is the first study of inter- and intraspecific satellite repeat variability, repeat expansions and correlations, as well as of male-biased repeats, in great apes.

Results

Repeat identification in short reads

To study inter- and intraspecific variability of satellite repeats in great apes, we utilized 100- or 150-base-pair (bp) Illumina sequencing reads generated for 79 individuals (57 females and 22 males; Table S1) as a part of the Ape Diversity Project (ADP) (Prado-Martinez et al. 2013). These included chimpanzees (Nigeria-Cameroon, Eastern, Central, and Western chimpanzees), bonobos, gorillas (Eastern lowland, Cross river, and Western lowland gorillas), Sumatran orangutans, and Bornean orangutans (Table S1). Additionally, in order to match the library preparation protocol that was used for these great ape data, we used sequencing reads for 9 human males from diverse populations generated as part of the Human Genome Diversity Project (HGDP) (Meyer et al. 2012; Cann et al. 2002; Rosenberg et al. 2002). After filtering (see Methods), median and mean numbers of reads per individual in this set of 79+9 = 88 samples were 43,663,219 and 43,782,069, respectively.

Sequencing reads are expected to present a more complete picture of satellite repeat distributions than the existing reference genome assemblies (Lower et al. 2018). To annotate repeats in sequencing reads, we used Tandem Repeats Finder, TRF (Benson 1999) (when available, 150-bp reads were trimmed to 100 bps for consistency) and focused on repeats with a repeated unit of ≤50 bp (so that at least two units could fit within a 100-bp read). Repeat motifs were phased alphabetically (see Methods). Additionally, we only retained sequencing reads in which repeated arrays covered at least 75% of the read length (i.e. at least 75 bp, see Methods) in order to exclude shorter repeated arrays that are unlikely to be present in heterochromatin. As a result, we identified 5,494 distinct repeated motifs (later called *satellite repeated motifs*, or *repeated motifs*) across the studied species and verified that they were not artifacts of read length or software choice (Supplementary Note 1).

Inter- and intraspecific variability

Repeat density varies among great ape species. We first compared the overall satellite repeat density (computed cumulating occurrences for all types of repeated motifs) among the studied ape species and

bioRxiv preprint doi: https://doi.org/10.1101/470054; this version posted November 18, 2018. The copyright holder for this preprint (which was not certified by peer review) is the author/funder, who has granted bioRxiv a license to display the preprint in perpetuity. It is made available under aCC-BY-NC-ND 4.0 International license.

subspecies (Fig. 1A). For each individual, *satellite repeat density* (later called *repeat density*) was computed as the total number of kilobases annotated in satellite repeats per million bases of sequencing reads (kb/Mb). Repeat density and sequencing depth were not correlated with each other (Fig. S1). PCR+ libraries were generated for ADP (Prado-Martinez et al. 2013) and HGDP (Meyer et al. 2012); while the types of repeated motifs identified were likely unaffected by the amplification step during library preparation, their densities could have been (Supplementary Note 2) and thus the precise repeat densities we report here might differ from the actual densities in the studied genomes (see also section on "Repeats in human trios" below, suggesting only minor effects of amplification on our repeat density estimation). However, because all samples were processed with the same library preparation protocol, we can compare the numbers among and within species (Fig. 1A). We observed the highest average repeat densities (across individuals) in Western and Eastern lowland gorillas (103 and 74.0 kb/Mb, respectively), and the lowest in human (11.9 kb/Mb) and Sumatran orangutan (22.6 kb/Mb).

Great ape genomes harbor only a handful of abundant repeated motifs, many of which are shared among species and are phylogenetically related. We next investigated whether great ape genomes possess a few highly abundant repeated motifs, or many different repeated motifs present at relatively low abundance. We ranked motifs by abundance and found that the six great ape species we considered (subspecies were combined for this analysis) contain only a small number of abundant repeated motifs: usually ≤12 in each of the species (Fig. S2). There were a total of 39 unique motifs in the set of 12 motifs x 6 species = 72 repeated motifs with density ranking 12 or higher in the six species analyzed (Fig. S2, Table S2). These 39 repeated motifs had overall average densities (across individuals) of 8.63 kb/Mb, 38.0 kb/Mb, 43.4 kb/Mb, 92.3 kb/Mb, 18.4 kb/Mb, and 27.1 kb/Mb in the six species (Fig. 1B), and represent approximately 73%, 90%, 82%, 94%, 81%, and 83% (i.e. very large portions) of the total satellite repeat density we found in the human, chimpanzee, bonobo, gorilla, Sumatran orangutan, and Bornean orangutan genomes, respectively.

The 39 abundant repeated motifs had various levels of sharing among species (Fig. 1B). Six motifs were present in all six species analyzed. The $(AATGG)_n$ repeat, shared by all six species, was the most abundant repeat in humans (with an average density of 6.63 kb/Mb) as well as in gorilla, bonobo, Sumatran orangutan, and Bornean orangutan (with average densities of 22.1 kb/Mb, 14.6 kb/Mb, 10.2 kb/Mb and 14.6 kb/Mb, respectively), and the second most abundant repeat in chimpanzee (with an average density of 5.53 kb/Mb). The next most abundant repeated motifs in human and orangutans were phylogenetically related to the $(AATGG)_n$ (Figs. 1B-C, Table S2). Their overall average densities (without the density of $(AATGG)_n$ itself) were 1.62 kb/Mb, 9.22 kb/Mb, and 13.7 kb/Mb in the genomes of human, Sumatran orangutan, and Bornean orangutan, respectively (Fig. 1B). In addition to $(AATGG)_n$ and repeated motifs related to it, we identified highly similar Subterminal Satellite (StSat) 32-mers (Royle, Baird, and Jeffreys 1994; Koga, Notohara, and Hirai 2011; Ventura et al. 2012) and a 31-mer related to

bioRxiv preprint doi: https://doi.org/10.1101/470054; this version posted November 18, 2018. The copyright holder for this preprint (which was not certified by peer review) is the author/funder, who has granted bioRxiv a license to display the preprint in perpetuity. It is made available under aCC-BY-NC-ND 4.0 International license.

them (all differing by 1-2 bases; Figs. 1B-C). These repeats were abundant in the genomes of chimpanzee, bonobo, and gorilla with overall average densities of 15.8 kb/Mb, 15.8 kb/Mb, and 39.6 kb/Mb, respectively. In fact, one of these 32-mers was the motif with the highest repeat density in chimpanzee (6.10 kb/Mb). 32-mers were absent from the human genomes analyzed, and were very sparse in the orangutan genomes (Fig. 1B). We found no relationship between the degree to which a repeated motif was shared across the six species and its repeat density (Fig. S3). In conclusion, the overall satellite repeat content in great ape genomes appears to be driven by only a few highly abundant repeated motifs, many of which are shared among species and are phylogenetically related to each other.

The majority of less abundant repeated motifs are species-specific. We subsequently analyzed the 5,455 repeated motifs constituted by the initial set minus the 39 abundant repeats discussed in the previous section, and found substantial differences among great ape species when profiling their presence/absence (Fig. S4B). Despite the relatively recent divergence of the species considered (Goodman, Grossman, and Wildman 2005), as many as 3,170 of the 5,455 distinct repeated motifs were species-specific. Among them, 2,312 were gorilla-specific, while only 262 were human-specific. As expected, the chimpanzee and bonobo sister species shared many repeated motifs (a total of 947, representing 75% and 78% of all repeats identified in each species, respectively), and so did the Sumatran and Bornean orangutan sister species (a total of 217, representing 99% and 97% of all repeats identified in each species, respectively). Interestingly, we found a positive relationship between the number of species-specific repeated motifs and mean repeat density in a species (Fig. S5; human is an outlier in this analysis). These results did not change qualitatively when we considered the same number of individuals per species (Figs. S6 and S4C-H).

Substantial differences exist among individuals, in repeat presence/absence as well as density. The majority of the 39 abundant motifs were present in all individuals of a given species (Fig. S4A) but exhibited substantial variability in repeat density among them (Table S3). For instance, the average fold difference for the $(AATGG)_n$ repeat among two unrelated human males in our study was 1.23. Other motifs, especially those of lower abundance, although identified in a species, were only present in a subset of individuals (Fig. S4B).

Relatedness of the studied species based on satellite repeat data. *(a) Individuals can be classified into species based on 14 unique, most abundant repeated motifs.* We investigated whether the densities of the 39 abundant repeats found across great ape genomes (Table S2) could separate individuals into species. We started with an exploratory Principal Component Analysis (PCA, Fig. 2A) of their densities. In the space of the first three components (which explain 98% of the variance; Table S4), individuals belonging to different species formed fairly well-separated groups. Next, we attempted to directly classify individuals into species. We found that using the densities of just 14 most abundant repeats (from the set

bioRxiv preprint doi: https://doi.org/10.1101/470054; this version posted November 18, 2018. The copyright holder for this preprint (which was not certified by peer review) is the author/funder, who has granted bioRxiv a license to display the preprint in perpetuity. It is made available under aCC-BY-NC-ND 4.0 International license.

of 39) already produced excellent classification performance; leave-one-out cross-validation resulted in accuracy of ~96% for a Linear Discriminant Analysis (LDA) classifier with uniform priors (Fig. 2B), and ~93% for a Random Forest classifier (Table S4). Using up to 20 most abundant repeats, the accuracy of LDA classification was as high as 97% (Fig. 2B).

(b) Hierarchical clustering based on repeat densities usually does not reproduce the accepted species phylogeny. Based on the results in (a) the question naturally arises of whether a hierarchical clustering of individuals would reproduce the accepted species phylogeny (Goodman et al., 2005). To address this, we computed distances between individuals based on Pearson and, separately, Spearman correlation coefficients – the latter being a more robust measure of similarity. Specifically, each individual was represented by a vector of repeat densities (for Pearson), or of ranks of such densities (for Spearman) and, for each pair of individuals, the correlation was calculated between their two vectors. For both these correlation types, we performed two separate analyses: (1) using all 5,494 unique repeated motifs; and (2) using the 39 abundant repeats. Also, two different linkage functions were used to implement the hierarchical clustering in each analysis and with each correlation type: “single” (which joins two clusters based on the minimal distance between individuals), and “complete” (which uses the maximal distance instead; see Methods). Interestingly, while species formed well-separated clusters (Fig. S7), the higher-level agglomeration only reproduced the accepted species phylogeny in scenarios where Pearson correlations and single linkage were used (on all, or on only the 39 abundant repeats; Figs. S7B,D). In contrast, using Pearson correlations and complete linkage, as well as using Spearman correlations and complete linkage, humans clustered with orangutans in both analyses (1) and (2) (Figs. 2C, S7A,C,E-G), contradicting the accepted species phylogeny. Lastly, using Spearman correlation and single linkage, orangutans, but not humans, clustered with gorilla and chimpanzee/bonobo, also contradicting the accepted species phylogeny (Fig. S7H).

(c) Phylogeny based on presence/absence of repeated motifs does not reproduce the accepted species phylogeny. We observed a similar pattern estimating a phylogeny based solely on the number of shared repeated motifs (in terms of their presence/absence). Chimpanzee, bonobo, and gorilla (sharing 717 repeated motifs) formed a cluster that did not include human (Fig. 2D, left), departing from the accepted great apes phylogeny (Fig. 2D, right). Note that many highly abundant repeats were also shared among chimpanzee, bonobo, and gorilla (Fig. 1B). In contrast, human, chimpanzee, and bonobo, while having a more recent common ancestor, shared as few as 14 repeated motifs (Fig. 2D). Taken together, both distances in repeat densities (Fig. 2C) and configurations of shared (vs. not shared) repeats (Fig. 2D) across species, show a distortion of the signals as compared with the accepted species phylogeny. This suggests an especially rapid evolution of satellite repeats among great apes.

bioRxiv preprint doi: https://doi.org/10.1101/470054; this version posted November 18, 2018. The copyright holder for this preprint (which was not certified by peer review) is the author/funder, who has granted bioRxiv a license to display the preprint in perpetuity. It is made available under aCC-BY-NC-ND 4.0 International license.

The densities of the 39 abundant repeats display high correlations, particularly for similar repeated motifs. Next, we computed Spearman correlation coefficients between pairs of repeats among the 39 abundant ones found in great apes genomes. Here, each repeat is represented by a vector of ranks for its densities across individuals (in each species). The significance of these correlations was tested against a chance background scenario simulated by random reshuffling of repeated motif labels (Figs. 3 and S8; see Methods). Most correlation coefficients were positive and rather large. Furthermore, we found that blocks with strong positive correlations tended to comprise phylogenetically related repeated motifs (Figs. 3 and 1C). Negative and moderately large coefficients (r<-0.5) were also observed (Fig. S8). In general, negative correlations were rare and mostly associated with the $(AAAG)_n$ repeat (Fig. S8).

The correlations between abundant repeats densities differed across great ape species. For example, in human, we observed many more positive correlations than expected by chance, but also a substantial number of negative correlations (Figs. 3A-B). In contrast, gorilla had a sizable subset of repeats with very high and significant positive correlations (coefficients >0.8), but very few negative correlations (Figs. 3C-D). Also interestingly, the two orangutan species displayed different patterns. In Sumatran orangutan, just as in human, we observed more positive than negative correlations – but none of the coefficients were significant. In Bornean orangutan, positive correlations were significant and negative correlations were not.

Male-biased repeats

Male-biased repeats are among the most abundant. We next focused on identifying repeats potentially located on great apes Y chromosomes, based on the expectation that they should be significantly more frequent in males than in females, i.e. male-biased. We considered all chimpanzee, bonobo and gorilla individuals, as well as ten orangutan individuals (combining five Sumatran and five Bornean). In addition to the nine human males from HGDP (Meyer et al. 2012; Cann et al. 2002; Rosenberg et al. 2002), we also used three fathers and three mothers from human trios (Table S1, see Methods). We restricted attention to repeated motifs with density above 0.5 kb/Mb in any given species. For each such motif we calculated the average male-to-female density ratio across individuals and assessed significance of the difference in repeat density between males and females with a Mann-Whitney test (Table S5). Since our sample sizes were relatively small, we used a high p-value cutoff (alpha=0.2) to compensate for lack of power – this, admittedly, increases the chances of false positives in our results. Our analysis resulted in a total of 18 significantly male-biased repeated motifs, which are candidates to be located on great apes Y chromosomes: one in human ($(AATGG)_n$), five in chimpanzee, nine in bonobo, fourteen in gorilla, and one in orangutans ($(ACTCC)_n$) (Table S5). Interestingly, all the significantly male-biased motifs were among the most abundant repeated motifs in the ape genomes (ranging between 1st and 14th in the species-specific ranks).

bioRxiv preprint doi: https://doi.org/10.1101/470054; this version posted November 18, 2018. The copyright holder for this preprint (which was not certified by peer review) is the author/funder, who has granted bioRxiv a license to display the preprint in perpetuity. It is made available under aCC-BY-NC-ND 4.0 International license.

Male-biased 32-mers can be found on the gorilla and bonobo Y chromosomes. We further restricted attention to male-biased 32-mers, which had higher incidence in males than females in chimpanzee, bonobo, and gorilla (Table S5), and searched for additional evidence that they indeed might be located on the Y chromosomes of these species. First, we screened the Y chromosome assemblies of chimpanzee (Hughes et al. 2010) and gorilla (Tomaszkiewicz et al. 2016) for occurrences of these male-biased 32-mers (see Methods; no bonobo Y chromosome assembly is currently available). We found them in the latter but not in the former. This could be explained by the fact that long PacBio reads, which are more likely to capture these 32-mers, were used to generate the gorilla's Y assembly, and not the chimpanzee's. However it is also possible that some of these 32-mers are indeed absent from the chimpanzee Y chromosome (see next paragraph).

Second, to experimentally assess whether male-biased 32-mers (Table S5) are present on the Y chromosomes of bonobo and chimpanzee, we performed FISH. We used two probes (see Methods); a degenerate probe containing the sequences of two male-biased 32-mers (Table S5), and a probe containing the flow-sorted bonobo Y chromosome. These probes were hybridized to metaphase spreads of bonobo and chimpanzee males. The 32-mer probe hybridized to (sub)telomeric locations of most chromosomes (Figs. 4A-B), suggesting an association with heterochromatin. Moreover, both probes hybridized to the bonobo Y chromosome, confirming Y localization (Fig. 4D) – consistent with our computational predictions (the p-values for bonobo male-to-female abundance differences were 0.03 and 0.05 for the two 32-mers included in the degenerate probe; Table S5). FISH could not confirm the presence of the same 32-mer probe on the chimpanzee Y chromosome (Fig. S9B) – again consistent with our computational analysis, which provided only weak evidence of male bias for the studied 32-mers in chimpanzee (p-values of 0.2 and 0.2 for the two 32-mers included in the degenerate probe; Table S5). In summary, we identified several male-biased repeats in the genomes of great ape species, and for a number of them we were able to validate their Y chromosome location either by examining Y assemblies or by FISH experiments.

Repeats in human trios

In order to investigate how the densities of satellite repeats change between generations, we studied them in three human trios. Two trios belonged to the CEU population (Utah Residents with Northern and Western European Ancestry) sequenced as a part of the Platinum Genomes (Eberle et al. 2017), and one belonged to the Ashkenazi Jews population (Zook et al. 2015). All nine samples were sequenced with a PCR-free protocol, providing a more unbiased view of repeat densities (Fig. 5A) compared to our larger data set (Fig. 1B). Remarkably, the densities of abundant repeats were similar between our PCR- and PCR+ human samples (Fig. 1B and Fig. 5A, respectively), suggesting that PCR amplification may have only minor effects on the repeat densities analyzed in our study.

bioRxiv preprint doi: https://doi.org/10.1101/470054; this version posted November 18, 2018. The copyright holder for this preprint (which was not certified by peer review) is the author/funder, who has granted bioRxiv a license to display the preprint in perpetuity. It is made available under aCC-BY-NC-ND 4.0 International license.

In each of the three trios we considered, we found a higher repeat density in men than women, in part due to the presence of the male-biased $(AATGG)_n$ repeat (Fig. 5B). Next, we investigated how much the repeat densities in children differed from those in their parents (Fig. 5C). For some of the repeated motifs, densities in children were within the range of parental values, but for others they were not. For autosomal satellites, based on random sampling of parental alleles, we expect children's densities to fall within the parental range 50% of the times. Interestingly, we observed that children's densities fell within the parental range for about two thirds of the 15 abundant motifs present in human (10/15, 11/15, 11/15 for each of the three families). Importantly, these included the same 10 repeats with children's densities within parental range for all three families, suggesting a shared constraint in their copy number in the human genome.

Estimating satellite repeat abundance and length with long-read data

Because short-read technologies can only provide information about total repeat abundances, and satellite repeats are routinely under-represented in sequenced assemblies, one can take advantage of long reads, e.g., as produced by Nanopore or PacBio, to provide a presumably less biased view of repeated array lengths. Unfortunately, adequate software to retrieve repeats from long sequencing reads, which are notoriously error-prone (with error rates around ~15-16% for both PacBio and Nanopore (Jain, Koren, et al. 2018; Rhoads and Au 2015)), does not currently exist. To address this limitation, we developed Noise-Cancelling Repeat Finder (NCRF; Harris et al., 2018, submitted), a stand-alone software that can recover repeat length distributions from long reads notwithstanding their high error rates. NCRF initially identifies continuous arrays of highly similar repeated motifs (imperfect repeats). Further, the composition of each such array is analyzed and the number of distinct motifs present in an array is computed alongside their frequencies. Each array is assigned to a motif that comprises more than 50% of that array. This is vital as arrays comprising a dominant motif and one or more derived motifs represent an important facet of biological variability (Plohl et al. 2008). Since the direct *de novo* identification of satellite repeats from error-prone long reads is challenging, we used the 39 abundant Illumina-derived repeated motifs identified above (see section 'Repeat identification in short reads') as queries for the screening of long reads by NCRF.

To evaluate densities and lengths of 39 Illumina-derived abundant motifs in long read technologies using NCRF, we sequenced six great ape individuals, one from each species of great apes, on one Nanopore MinION flow cell (Table S6-7), and employed publicly available PacBio sequencing reads available for four great ape species (Table S6 and S9)(Gordon et al. 2016; Kronenberg et al. 2018). For our Nanopore data, the longest observed read was 206 kb and the read length N50 ranged from 26 to 37 kb among samples (Table S7). In comparison, using a single flow cell of PacBio data for each species, the longest observed read was 184 kb and the read length N50 ranged from 19 to 34 kb among samples (Table S8).

bioRxiv preprint doi: https://doi.org/10.1101/470054; this version posted November 18, 2018. The copyright holder for this preprint (which was not certified by peer review) is the author/funder, who has granted bioRxiv a license to display the preprint in perpetuity. It is made available under aCC-BY-NC-ND 4.0 International license.

Concerning repeat densities we found with NCRF (Fig. 6), for both PacBio and Nanopore reads, the general patterns were consistent with those inferred from Illumina reads with TRF (Fig. 1B) – however the exact densities differed. Interestingly, some of the repeated motifs abundant in short-read data, such as the $(AATGG)_n$ repeat, were not as abundant in long-read data.

We also found that long satellite arrays were frequently a mix of more than one motif, present in perfect patches interspersed with highly similar, yet different, sequences. To come to this conclusion, we proceeded as follows. First, we calculated lengths for each of the 39 abundant repeated motifs in each species. Next, we verified that long reads were able to capture the full lengths of satellite repeats (Figs. S10-S11), as demonstrated by the fact that in the majority of cases long reads encompassed complete repeat arrays (depending on the species, 90-95% and 99% of repeat arrays were nested within individual reads in Nanopore and PacBio, respectively, Table S9). In Nanopore, the median lengths ranged from 76 bp up to 7.3 kb (Table S10, Fig. S10). The longest repeat arrays we recovered were for $(AATGG)_n$ and 32-mers (Fig. 7), some of which were over 59 kb (Table S10). Last, we focused on the arrays with a single dominant motif and, depending on the species, found that at least 10-25% of all arrays were composed of a mix of different repeated motifs (Table S11). This is likely an underestimation, as we only detected overlaps in repeat annotations among the 39 most abundant repeated motifs. In PacBio, the available reads from human, chimpanzee, gorilla, and Sumatran orangutan resulted in median repeat array lengths ranging from 76 bp up to 0.8 kb (Table S10, Fig. S11). The longest repeat arrays we recovered with PacBio were over 17 kb (Table S10). Taken together, our results suggest frequent interspersion of perfect repeats with highly similar repeated motifs.

Discussion

Satellite repeats constitute a large portion of the human genome (Jain, Koren, et al. 2018; Spinelli 2003), yet they have been routinely underexplored in the genomes of great apes (Kronenberg et al. 2018). Our study fills this gap; it provides a detailed characterization of this important component of hominid genomes and demonstrates a remarkable divergence of satellite repeats among ape species separated by less than 14 MY (Glazko and Nei 2003).

Satellite repeats in great ape genomes

The $(AATGG)_n$ repeat and its derivatives. Previous studies investigated the variability, abundance, and length distribution of the $(AATGG)_n$ repeat in the human genome (Tagarro et al. 1994; Skaletsky et al. 2003; Altemose et al. 2014; Subramanian et al. 2003), but not in great apes. This repeat is the source of Human Satellites 2 and 3 (HSat2 and HSat3)(Altemose et al. 2014). It was also identified in orangutan, chicken, maize, sea urchin, and *Daphnia* (Grady et al. 1992; Flynn et al. 2017). We determined this repeat to be abundant in great ape species. Independent of sequencing technology used, its density was

bioRxiv preprint doi: https://doi.org/10.1101/470054; this version posted November 18, 2018. The copyright holder for this preprint (which was not certified by peer review) is the author/funder, who has granted bioRxiv a license to display the preprint in perpetuity. It is made available under aCC-BY-NC-ND 4.0 International license.

usually highest in gorilla (second highest with Nanopore), rather high in orangutans, human, and bonobo, and lowest in chimpanzee (Figs. 1B and 6). This is in agreement with a suggestion that, during primate evolution, HSat3 amplification peaked in gorilla and orangutan lineages (Jarmuż et al. 2007). We also found high intraspecific variability in the density of $(AATGG)_n$, sometimes reaching up to 1.51-fold pairwise difference between individuals of the same species (Table S3). Similarly, in human trios, its density in children differed from that in their parents by up to 1.25-fold (Table S12). These findings strongly argue for the rapid evolution of this repeat.

We found that $(AATGG)_n$ is ubiquitously present in all great ape individuals in our study, suggesting that it performs an important function. It is located at pericentromeric regions of acrocentric chromosomes (Lee et al. 1997), can fold into a non-B DNA conformation (Grady et al. 1992; Zhu et al. 1996; Chou et al. 2003), and was suggested to participate in forming centromeres (Grady et al. 1992). Importantly, under conditions of stress, the $(AATGG)_n$ repeat is transcribed from three to four 9q12 loci into long noncoding RNAs which, together with several proteins, form nuclear stress bodies and play a critical role in heat shock response (Nakahori et al. 1986; Jolly et al. 2004; Goenka et al. 2016; Biamonti and Vourc'h 2010). In fact, such RNAs were recently shown to be required to "provide full protection against the heat-shock-induced cell death" via contributing to transcriptional silencing (Goenka et al. 2016). Thus, these $(AATGG)_n$ repeat-bearing loci on chromosome 9 are essential for heat shock response. Some of the RNAs transcribed from them can be very long (Jolly et al. 2004), with polyadenylated transcripts ranging from 2 to >5 kb (Goenka et al. 2016). In agreement with this observation, we found that some $(AATGG)_n$ imperfect arrays, which can be part of these transcripts, can be over 59 kb long. Most of our study is based on raw read analysis and does not provide chromosome-level resolution, thus we could not determine which arrays originated from chromosome 9.

Our study has also identified abundant repeated motifs that were derived from $(AATGG)_n$ (Figs. 1B-C). Interestingly, some of them, including the $(AATGG)_n$ repeat itself, are matching substrings of the most common 24-mers indicative of a specific HSat subfamily (Altemose et al. 2014) — either with no mismatches (AATGG, ACTCC, and AAAG) or with one mismatch (AATGGAATGGAGTGG, AATGGAGTGG, AATGGAATGTG, AATCGAATGGAATGG). This provides an independent confirmation that they form satellite repeats.

Subterminal Satellites. Another interesting group of satellite repeats highlighted by our study are the phylogenetically related, AT-rich 32-mers. These are called Subterminal satellites (StSats) because, as demonstrated by our and other studies (Royle, Baird, and Jeffreys 1994; Ventura et al. 2012), their location is proximal to telomeres. Independent of the sequencing technology used, we found that these repeats are highly abundant in gorilla, still very abundant in chimpanzee and bonobo, but absent in human. These findings corroborate early studies hypothesizing that these repeats were present in the common ancestor of hominids (albeit in small amounts), and then lost in the human lineage (Ventura et

bioRxiv preprint doi: https://doi.org/10.1101/470054; this version posted November 18, 2018. The copyright holder for this preprint (which was not certified by peer review) is the author/funder, who has granted bioRxiv a license to display the preprint in perpetuity. It is made available under aCC-BY-NC-ND 4.0 International license.

al. 2012; Royle, Baird, and Jeffreys 1994; Koga, Notohara, and Hirai 2011). The loss of StSats in orangutans was also proposed (Ventura et al. 2012; Royle, Baird, and Jeffreys 1994; Koga, Notohara, and Hirai 2011), however our analysis suggests that such loss was incomplete, as we can still find StSat traces in orangutan genomes using both Illumina and Nanopore read data. Consistent with the notion of a partial loss in orangutans, StSats are polymorphic in their presence/absence among orangutan individuals (Fig. S4A). In contrast, the majority of StSats are present in all gorilla, chimpanzee and bonobo individuals analyzed, suggesting that they might be functionally important in their genomes. Various roles for StSats have been proposed, including participation in meiosis (Ventura et al. 2012; Royle, Baird, and Jeffreys 1994; Koga, Notohara, and Hirai 2011), telomere clustering and metabolism, as well as the regulation of replication timing in the vicinity of telomeres (Novo et al. 2013).

Male-biased repeats. Leveraging differences in repeat density between males and females, we identified 18 candidate male-biased repeats in great apes (Table S5). These included the $(AATGG)_n$ repeat, which was previously shown to be present on the human Y chromosome as the primary repeated unit of its three common satellites (DYZ1, DYZ17, and DYZ18) (Skaletsky et al. 2003; Kunkel et al. 1976), and on the Y chromosome of orangutan, gorilla and chimpanzee/bonobo with FISH (Jarmuz et al. 2007). Our analysis of human trios also confirmed that this repeat is located on the Y chromosome; we observed higher densities in males than females, and greater differences in density between parents and children of different sex (up to 1.25-fold), than of the same sex (up to 1.06-fold; Table S12). Additionally, we found several StSats to be male-biased and confirmed their presence in the gorilla Y assembly and in the bonobo Y chromosome using FISH (Fig. 4). This substantially increases the current knowledge of both candidate and validated Y chromosome heterochromatic repeats in great apes. Prior to our study, these repeats were underexplored because only human, chimpanzee and gorilla Y chromosome assemblies are currently available and such assemblies are mostly euchromatic (Skaletsky et al. 2003; Hughes et al. 2010; Tomaszkiewicz et al. 2016).

Differences in heterochromatin density can be one of the major contributors to the dramatic length differences observed among the Y chromosomes of great apes (Gläser et al. 1998; Hughes et al. 2010). To shed light on this, we tested whether the differences in satellite repeat content between males and females, presumably reflecting the Y chromosome repeat content, corresponds to the differences in lengths of great ape Y chromosomes. For instance, the difference in content of male-biased satellite repeats between males and females is 13.1, 8.0 and 2.5 kb/Mb for gorilla, bonobo, and chimpanzee, respectively (Table S13). In agreement with the order of these values, cytogenetic estimates indicate that, among the Y chromosomes of these three species, the gorilla's is the longest Y chromosome, the bonobo's is intermediate, and the chimpanzee's is the shortest (Gläser et al. 1998). Therefore, satellite repeats may indeed be playing an important role in determining Y chromosome length variation in great apes. However, they are likely not the sole contributors; indeed, the difference in satellite repeat content

bioRxiv preprint doi: https://doi.org/10.1101/470054; this version posted November 18, 2018. The copyright holder for this preprint (which was not certified by peer review) is the author/funder, who has granted bioRxiv a license to display the preprint in perpetuity. It is made available under aCC-BY-NC-ND 4.0 International license.

between males and females for humans is only 2.0 kb/Mb, despite the fact that the human Y chromosome falls between bonobo's and gorilla's in length (Gläser et al. 1998).

It was proposed that enrichment of different, or accumulation of unique, satellite DNA is the first step in separation of the X and Y chromosomes (Brutlag 1980). It was also hypothesized that the composition of the heterochromatin on the Y may differ from that on other chromosomes because of (1) absence of recombination; (2) a potential role of heterochromatin in silencing the Y; and (3) the small effective population size of the Y (Bachtrog 2013; Nei 1970; Charlesworth and Charlesworth 2000). Consistent with these hypotheses, some *Drosophila* species (*D. virilis*, *D. melanogaster*, *D. simulans*, and *D. sechellia*) exhibited many Y-enriched or Y-specific satellite repeats (Wei et al. 2018). In contrast, other *Drosophila* species (*D. pseudoobscura* and *D. persimilis*) instead have prominent transposable element (TE) abundance on the Y (Wei et al. 2018) — suggesting that Y chromosome degeneration occurs by satellite repeat accumulation in some species, and TE accumulation in others. These two alternatives can be explored also for the great ape Y chromosomes, once their additional assemblies become available.

The Y chromosome heterochromatin is a major source of epigenetic regulation, modulating phenotypic variation in natural populations (Lemos, Branco, and Hartl 2010). For instance, in *Drosophila*, its content and length affect expression of autosomal genes (Lemos, Araripe, and Hartl 2008). Similarly, a repeat-rich non-coding RNA was recently found to play a role in regulating the expression of several genes in mouse testis (Reddy et al. 2018). Such a phenomenon in primates is yet to be investigated.

Co-occurrence of satellite repeats. Our observations suggest dependencies among the densities of many repeated motifs, and an underlying structure in their distribution in the great apes genomes – which is at least partially dictated by sequence similarity and evolution, stemming from the interspersion of longer satellite arrays with similar motifs. This echoes recent observations made for *Drosophila* (Wei et al. 2014, 2018) and *Chlamydomonas reinhardtii* (Flynn et al. 2018). Similarly to the pattern observed in *Drosophila*, in great apes clusters of co-occurring repeats are in part driven by their sequence similarity. Several hypotheses were proposed to explain such a pattern; for instance, several similar repeat motifs can serve as recognition sites for the same DNA-binding proteins (Wei et al. 2014), and correlated motifs might be physically linked to each other due to a large-scale duplication or due to interspersion. An example of interspersion are two groups of HSat3 DNA: the first group is dominated by $(AATGG)_n$ and the second group represents a mix of $(AATGG)_n$ and $(ACTCC)_n$ (Jarmuż et al. 2007). We also found antagonistic relationships among some repeats, in particular among $(AAAG)_n$ and several other repeats. Again similar to observations made in *Drosophila* (Wei et al. 2014), this can occur when the expansion of one repeat type comes at the expense of another. The differences we found in nature and strength of dependencies among repeat densities in various great apes might be explained by differences in the overall tolerance their genomes have towards repetitive load. Future studies can incorporate data on

bioRxiv preprint doi: https://doi.org/10.1101/470054; this version posted November 18, 2018. The copyright holder for this preprint (which was not certified by peer review) is the author/funder, who has granted bioRxiv a license to display the preprint in perpetuity. It is made available under aCC-BY-NC-ND 4.0 International license.

long-distance genome interactions (e.g., Hi-C) to further explore repeat co-occurrence patterns in great ape genomes.

Interspecific differences and lack of phylogenetic signal in repeat densities

We found drastic differences among great ape species in overall repeat content. Independent of the sequencing technology used, overall repeat density was highest in gorilla, intermediate in chimpanzee and bonobo, and lowest in human and orangutans (Figs. 1B and 6). This is primarily explained by the absence or paucity of StSats in human and orangutans, respectively. Also, while clustering based on repeat densities did correctly assign individuals into species, subsequent agglomeration did not follow the expected species phylogeny. In particular, we frequently observed chimpanzee, bonobo, and gorilla clustering together, and human clustering with orangutan (Fig. 2C). We found that similarities among chimpanzee, gorilla and bonobo individuals (Figs. S7F-H) were in part driven by StSats (data not shown) — but in certain instances they clustered together even after the exclusion of such repeats (Fig. S7I). Several explanations are possible for this unexpected observation, including incomplete lineage sorting (Kronenberg et al. 2018), parallel gains of the same repeats along different lineages, molecular drive, and segregation distortion (reviewed in (Wei et al. 2018)). Future studies should examine each of these explanations in detail. At present, what is clear is that satellite repeats have a notably high tempo of turnover and, at least at the timescale resolution of great ape evolution, do not carry phylogenetic signals. Interestingly, our results are more similar to those found for Drosophila populations than for Drosophila species (Wei et al. 2014; Wei et al. 2018).

The power of long reads, study limitations, and future directions

One of the strengths of our study is in that we combined information from three different sequencing technologies to investigate satellite repeats. We identified repeated motifs from rather accurate short-read (Illumina) data, and augmented information about them using long reads from the Nanopore and PacBio platforms. Critically, we studied satellite repeats from sequencing *reads*, and not from *reference genomes*, thus greatly expanding our current knowledge about yet unassembled portions of great ape genomes. The use of data from long reads has allowed us to gain reliable information on repeat length. Indeed, depending on the species and technology, 90 to 99% of the repeat arrays in our study were wholly contained within single sequencing reads (Table S9). The longest repeat arrays were 59 kb and 17 kb in length, as identified using the Nanopore and PacBio platforms, respectively. Such lengths are unprecedented; the recent PacBio-augmented assembly of the sooty mangabey (a primate) identified a 52-kb repeat array, and this was the longest found in an analysis comprising as many as 719 assembled eukaryotic genomes (Surabhi et al. 2018). Our study confirms that long-read technologies are indeed suitable for the analysis of long heterochromatic satellites. This is due both to their progressively increasing read lengths, and to recent advances in the algorithms used to tackle their noisy error profiles,

bioRxiv preprint doi: https://doi.org/10.1101/470054; this version posted November 18, 2018. The copyright holder for this preprint (which was not certified by peer review) is the author/funder, who has granted bioRxiv a license to display the preprint in perpetuity. It is made available under aCC-BY-NC-ND 4.0 International license.

e.g., NCRF (Harris et al. 2018 submitted). Deciphering repeat lengths and structures will enable genotyping and assigning potential functions to a larger set of repeat arrays than previously possible. For example, Sonay and colleagues showed gene expression divergence between human and great apes to be higher for genes that encompassed tandem repeats (TRs) (Sonay et al. 2015). However, since their study required TRs to be fully encompassed within short Illumina sequencing reads, they were able to analyze only 58% of TRs present in the human reference. Nanopore sequencing was recently used to characterize the first complete human centromere on the Y chromosome (Jain, Olsen, et al. 2018) and to determine the lengths of human telomeric repeats (Jain, Koren, et al. 2018). We expect a growing interest in tools and approaches operating directly on raw, ultra-long reads (Lower et al. 2018).

Many of our conclusions are robust to the use of sequencing technology. However, we did find differences in the exact values of repeat density estimates obtained from the three technologies we considered. These differences could be due to the vastly different library preparation and sequencing protocols. While Illumina reads always represent short fragmented DNA, long DNA molecules used for PacBio and Nanopore sequencing could form secondary structures. We have recently shown that non-B DNA structures can affect PacBio sequencing depth (Guiblet et al. 2018). For Nanopore, fragments harboring these structures might not pass through the pores. In both cases, the representation of repeats capable of forming non-B DNA might be altered. This, for instance, might explain at least in part why the $(AATGG)_n$ repeat, known to form a non-B DNA structure (Grady et al. 1992), is underrepresented in Nanopore and PacBio vs. Illumina data (Figs. 1B and 6). Furthermore, sequence context matters; the stability of a DNA fragment and its propensity towards different types of DNA damage was shown to depend on its nucleotide composition (Wei et al. 1998; Melvin et al. 1994; Lim et al. 2006; Costello et al. 2013). Moreover, different genome k-mers are not represented equally in Nanopore sequencing, an issue that is being mitigated by advances in the Nanopore base calling algorithms (Lu, Giordano, and Ning 2016; Ip et al. 2015). The Illumina short-read sequencing used in the first part of our study might have its own issues. The APD and HGDP sequencing libraries we analyzed were generated with the PCR+ protocol. This might have led to an overestimation of repeat densities or difficulties with sequencing of the extremely GC-rich fragments. However, human repeat densities were very similar when estimated from PCR+ vs. PCR- samples (Figs. 1B and 5A), and we observed each repeat motif at each locus to be affected by PCR amplification at approximately the same rate (Supplementary Note 2). In *Drosophila* (Wei et al. 2018), omission of the PCR step improved correlation of satellite abundances between replicates. It is much more expensive to generate PCR- data on a large scale in apes than in *Drosophila*, especially when intraspecific variation, and thus multiple individuals, are of interest. However, such data should definitely be generated for great apes in the future. In this study, we did not perform the GC-bias correction (Benjamini and Speed 2012) that was employed in some other studies (e.g., Flynn et al. 2017; Wei et al. 2018). Available GC-correction pipelines require reference genomes and are thus unsuitable for

bioRxiv preprint doi: https://doi.org/10.1101/470054; this version posted November 18, 2018. The copyright holder for this preprint (which was not certified by peer review) is the author/funder, who has granted bioRxiv a license to display the preprint in perpetuity. It is made available under aCC-BY-NC-ND 4.0 International license.

whole-genome sequencing reads with suboptimal or missing references (e.g., for Y chromosomes in most apes).

The conclusions of our study are limited by the shortcomings of ADP (Prado-Martinez et al. 2013), e.g., by small sample sizes, as well as by skewed male-to-female ratios, for some species (particularly for orangutans). The variability we observe among individuals is much more striking than could possibly be explained by differences between wild-born and captive subjects (the latter are present in small numbers in the ADP), and by cross-sample contamination (known to be present at ADP). The sex of individuals also contributed to differences in repeat densities. Batch effects between ADP and HGDP studies might also be reflected in our data, however our results for humans were robust to the use of PCR+ and PCR- protocols.

Our study focused on relatively short repeated units (<50-bp), because we identified satellite repeats from short reads (two 50-bp repeats fit a 100-bp read). Our use of such short-motif repeats as a proxy for heterochromatin is justified based on several considerations: (1) they are part of long arrays, as identified by long-read data; (2) some of them match to 24-mers differentiating HSat families (Altemose 2014); and (3) some of them have (sub)telomeric locations, as demonstrated by our FISH experiments (Fig. 4). Repeats with longer units were not considered because the computational tools to identify them *de novo* in noisy long reads do not currently exist. Some studies focused on the analysis of the 171-bp centromeric heterochromatic arrays whose sequence in the human genome has been well characterized (Jain, Olsen, et al. 2018; Miga et al. 2014; Melters et al. 2013). Analyzing repeats with longer repeat units in great apes will be of great interest for future studies, once algorithms to reliably identify novel repeats from long reads are developed.

Conclusions

Our study represents the first detailed genome-wide investigation of heterochromatin turnover among great apes, characterizing species as well as sex differences based on information obtained from both short- and long-read sequencing data.

Methods

Sequencing data and quality filtering. From the ADP (Prado-Martinez et al. 2013), we focused on 399 fastq files with forward reads because they surpassed those with reverse reads in both sample size and quality (the latter was computed using FastQC v0.11.2 for all files using 10 randomly selected reads per file). Ape individuals sequenced in multiple Illumina sequencing runs were kept separately for all the

bioRxiv preprint doi: https://doi.org/10.1101/470054; this version posted November 18, 2018. The copyright holder for this preprint (which was not certified by peer review) is the author/funder, who has granted bioRxiv a license to display the preprint in perpetuity. It is made available under aCC-BY-NC-ND 4.0 International license.

downstream processing and treated as technical replicates. Excluding 39 files with read lengths shorter than 52 bp resulted in 360 files (322, 32, and 6 files with read lengths 100 bp, 101 bp, and 151 bp, respectively). Subsequently, excluding 51 files with read counts smaller than 20,000,000 (to avoid potential sampling bias resulting from low read counts) resulted in 309 files. The files belonging to genetically close relatives to other samples (Bulera, Kowali, Suzie and Oko)(Prado-Martinez et al. 2013) were also removed, resulting in 295 fastq files. To avoid sequence bias revealed by QC analysis (over-represented k-mers present profusely toward read ends), we discarded all reads that contained at least one base pair with a Phred quality score below 20 using FASTX-Toolkit (version 0.0.13, fastq_quality_filter -Q33 -v -q 20 -p 100).

Identification of Repeats. Reads retained after such filtering were converted from fastq to fasta format and repeats in them were identified with TRF (version trf409.legacylinux64, parameters MATCH=2 MISMATCH=7 DELTA=7 PM=80 PI=10 MINSCORE=50 MAXPERIOD=2000 -l 6 -f -d -h -ngs) (Benson 1999). The resulting repeats were parsed using the script parseTRFngs.py that implements collapsing of the same group of repeats (shifts and reverse complements) into a single representative. We required each repeat array to be at least 75 bp in length. Finally, instead of using all technical replicates for a given individual, we utilized median values (among replicates) of densities reported in kb/Mb for each repeated motif. To verify that the technical replicates of the same individual were consistent in their repeat estimates, we calculated the tightness of their estimates or intraclass (between technical replicates) correlation coefficient (using R package ICCbare) for the 100 most abundant repeats. Median intraclass correlation coefficient was 0.96 (Fig. S12).

To avoid duplicates in the output, the recovered repeats were further filtered and formatted. Namely, we merged all repeats that shared the basic repeated unit and were in close vicinity (less than the minimal unit length of the two neighboring repeats) to each other. Reads containing the same repeated motif can map to either reference or reverse strand, and the annotated repeats can start with a different leading nucleotide. Thus, we report the data on occurrences of a repeated motif whose phase was chosen alphabetically, and combine the data for motifs and their reverse complement sequences. Because the same long stretches of repeats can have different beginnings (e.g. AATGG and ATGGA differ by a 1-bp shift) or can be present on different strands (e.g. AATGG and CCATT), we reformatted all repeats into the lexicographically smallest rotations. This means that for all possible rotations (1-bp shift followed by 1-bp increments of shift size up to the unit length) and both possible strands, we picked only one representative. This representative is the first repeat in alphabetical order out of all generated possibilities that we described above.

Calculation of repeat frequency and density. We required each repeated motif to be present at $\geq$100 loci per 20 million reads. For repeated motifs that passed these filters, we calculated the corresponding

bioRxiv preprint doi: https://doi.org/10.1101/470054; this version posted November 18, 2018. The copyright holder for this preprint (which was not certified by peer review) is the author/funder, who has granted bioRxiv a license to display the preprint in perpetuity. It is made available under aCC-BY-NC-ND 4.0 International license.

repeat densities after normalizing for the read length and the read count after filtering. To calculate repeat density for each species, we included only those repeats that were present in at least one individual of that species.

Correlations of repeat co-occurrences. To assess the significance of observed correlations of repeat motifs (using Spearman coefficient and ranks based on the repeat density), we generated 10 reshuffled datasets of the original repeat densities of 39 abundant repeats separately for each species (visualized as grey band in Fig. 3). Reshuffling was done as follows: in a matrix of individuals x repeats, we kept the content of the matrix, but randomly reassigned column names, so that the biological associations among repeats were broken and those occurring were due to chance.

The sequence similarity and inter-relatedness among the 39 most abundant repeated motifs. The sequence similarity was calculated using MEGA7 (Kumar et al. 2016). Only substitutions (and not insertions or deletions) were considered. The pairwise distances were calculated using the number of differences (both transitions and transversions) and treating gaps with pairwise deletion. For each species, we calculated mean repeat density across all individuals.

Length distribution for long reads. Repeated motifs were identified in long reads using NoiseCancelingRepeatFinder, version 0.09.03 (Harris et al., 2018, submitted). The current version of the algorithm can be downloaded from: github.com/makovalab-psu/NoiseCancellingRepeatFinder/. For more detailed information on how to run the program, see Supplementary Note 4. For PacBio and Nanopore sequencing, --scoring=pacbio (M=10 MM=35 IO=33 IX=21 DO=6 DX=28) and --scoring=nanopore (M=10 MM=63 IO=51 IX=98 DO=27 DX=34) options were used, respectively. The maxnoise parameter was set to 20% to retain long reads with noisy repeat arrays. Subsequently, the repeated arrays were analyzed for their motif composition and each array was assigned to a motif that comprises more than 50% of an array.

Experimental validations of the male-biased repeats

Preparation of the probes. The whole bonobo Y chromosome painting probe (WBY) was prepared from flow-sorted bonobo Y chromosomes and labeled with biotin-16-dUTP (Jena BioScience) using DOP-PCR according to (Yang et al. 2009). Oligonucleotide probe (Pan32) (/5AmMC12/ATCTGTATAAACATGGAAATATCTACACCGCY) was prepared and labeled using Alexa Fluor oligonucleotide amine labeling kit (Invitrogen).

FISH. Metaphases were prepared from chimpanzee male and female lymphoblastoid cell line and from bonobo male fibroblast cell line following a standard protocol of colcemid treatment, hypotonization and methanol/acetic acid fixation (Howe, Umrigar, and Tsien 2014). Slides were pre-treated with acetone for

bioRxiv preprint doi: https://doi.org/10.1101/470054; this version posted November 18, 2018. The copyright holder for this preprint (which was not certified by peer review) is the author/funder, who has granted bioRxiv a license to display the preprint in perpetuity. It is made available under aCC-BY-NC-ND 4.0 International license.

10 min and aged at 65°C for 1 h. Subsequently, the slides were denatured in the alkaline solution (Sigma) for 5 min, followed by neutralization in 1M Tris-HCl, pH 7.5, and one wash in 1x PBS for 4 min. Next, a series of dehydration washes were performed as follows: 70% EtOH at -20°C for 4 min, 70% EtOH for 2 min, 90% EtOH for 2 min, and 100% EtOH for 4 min. The WBY probe was denatured in hybridization buffer at 75°C for 15 min and pre-annealed at 37°C for 30 min. Subsequently, 25 ng of the Pan32 probe was applied to the hybridization area and incubated at 37°C for 12 h for chimpanzee male chromosomes as well as for bonobo male chromosomes. In a separate FISH experiment, the mix of 25 ng of WBY and 25 ng of Pan32 was applied to the hybridization area and incubated at 37°C for 24 h for bonobo male chromosomes and for 48 h for chimpanzee male and female chromosomes (cross-species FISH). Post-hybridization washes were performed in 0.5x SSC at 50°C for 5 min, 2x SSCT at 37°C for 5 min, and 1x PBS at at 37°C for 5 min. For slides with the mix of probes, an additional step of probe detection with Cy3-Streptavidin (Sigma) was applied. Slides were stained with DAPI (Vector Laboratories) and visualized under the Keyence BZ-9000 fluorescence microscope. Photodocumentation was performed using the 100x immersion objective and the images were analyzed using BZ-Viewer and BZ Analyzer.

Nanopore library preparation and sequencing. DNA was extracted from male cell lines of bonobo (AG05253, Coriell Institute), gorilla (KB3781, “Jim”, San Diego Zoological Society), Bornean orangutan (AG05252, Coriell Institute), and Sumatran orangutan (AG06213, Coriell Institute) using the MagAttract High Molecular Weight DNA Kit (Qiagen, Germany). Male chimpanzee DNA sample (CH159, “Rock”) was provided by Dr. Mark Shriver and was acquired from the Bastrop Research Center. Human male DNA (J101) was provided by the University of Chicago.

Residual RNA was removed by digesting 3.5 µg of extracted DNA with 10 µg RNase A (Amresco) at 37 °C for 1 h, followed by purification with 1 volume of AMPure XP beads (Beckman Coulter). DNA integrity was visualized on a 0.5% agarose gel, DNA purity was determined with NanoDrop, and the concentration was measured with a Qubit broad-range assay. Libraries were prepared with the Native Barcoding Kit 1D (PCR-free) and the Ligation Sequencing Kit 1D (Nanopore) starting with 2 µg DNA per sample. DNA repair and end-repair were combined in one step as described in the 1D gDNA long reads without BluePippin protocol (version: GLRE_9052_v108_revB_19Dec2017; updated: 10/01/2018). Barcoding and adapter ligation were performed as indicated in the 1D Native barcoding genomic DNA (with EXP-NBD103 and SQK-LSK108) protocol (version: NBE_9006_v103_revP_21Dec2016; updated: 16/02/2018), starting with 700 ng of end-prepped DNA per sample. 250 ng of barcoded DNA per sample were pooled and all further steps were performed according to the 1D gDNA long reads without BluePippin protocol. DNA low-binding tubes as well as wide-pore low-retention pipette tips were used for DNA handling in all steps. Sequencing was performed with a MinION using a flow cell of the type FLO-MIN106 - R9.4 for 48 h. This resulted in 396, 55, 667, 526, 615 and 383 Mb of data (distributed among 26, 4, 43, 36, 40, and 22

bioRxiv preprint doi: https://doi.org/10.1101/470054; this version posted November 18, 2018. The copyright holder for this preprint (which was not certified by peer review) is the author/funder, who has granted bioRxiv a license to display the preprint in perpetuity. It is made available under aCC-BY-NC-ND 4.0 International license.

thousand reads) for human, chimpanzee, bonobo, gorilla, Sumatran and Bornean orangutan, respectively.

Declarations

Ethics approval and consent to participate

The human individual (J101) provided informed consent.

Consent for publication

Not applicable.

Availability of data and material

Illumina sequencing reads from 79 great apes were part of the Ape Diversity Project (Prado-Martinez et al. 2013). Sequencing reads generated for human populations were generated by (Meyer et al. 2012) Additionally, human samples from the Genome in a Bottle project (Zook et al. 2015) and two human trios from 1000 Genomes Project (1000 Genomes Project Consortium et al. 2015) — with ids HG002, HG003, HG004, NA12889, NA12890, NA12877 and NA12891, NA12892, NA12878, respectively(1000 Genomes Project Consortium et al. 2015) — were used. The publicly available PacBio data had following ids: SRR2097942 for human, SRR5269473 for chimpanzee, ERR1294100 for gorilla, and SRR5235143 for Sumatran orangutan. The Nanopore data generated are deposited under the BioProject SUB4784337. All scripts available from the git repository are at https://github.com/makovalab-psu/heterochromatin.

Competing interests

The authors declare that they have no competing interests.

Funding

Funding was provided by the Eberly College of Sciences, The Huck Institute of Life Sciences , and the Institute for CyberScience, at Penn State, as well as, in part, under grants from the Pennsylvania Department of Health using Tobacco Settlement and CURE Funds. The department specifically disclaims any responsibility for any analyses, responsibility, or conclusions.

bioRxiv preprint doi: https://doi.org/10.1101/470054; this version posted November 18, 2018. The copyright holder for this preprint (which was not certified by peer review) is the author/funder, who has granted bioRxiv a license to display the preprint in perpetuity. It is made available under aCC-BY-NC-ND 4.0 International license.

Authors' contributions

The study was conceived and designed by MC and KDM. MC performed the bioinformatics analysis. MT performed FISH experiments, RSH implemented NCRF and assisted with computational analysis of long reads, and BA performed Nanopore sequencing. FCH advised with the statistical parts of the paper. The manuscript was written by MC and edited by FCH and KDM. All authors read and approved the manuscript.

Acknowledgments

We thank Wilfried Guiblet and Arslan Zaidi for valuable biological insights, and Marzia Cremona for statistical advice. We are grateful to Kate Anthony for DNA extractions for Nanopore sequencing; Oliver Ryder and San Diego Zoological Society for providing gorilla cell line; Mark Shriver for providing the male chimpanzee sample; Malcolm Ferguson-Smith and Jorge Pereira for providing the flow-sorted bonobo Y chromosome material; Jorge Pereira and Laura Carrell for advice on FISH experiments; and Laura Carrel and Shaun Mahony for critical reading of the manuscript

References

1000 Genomes Project Consortium, Adam Auton, Lisa D. Brooks, Richard M. Durbin, Erik P. Garrison, Hyun Min Kang, Jan O. Korbel, et al. 2015. “A Global Reference for Human Genetic Variation.” *Nature* 526 (7571): 68–74.

Allshire, R. C., E. R. Nimmo, K. Ekwall, J. P. Javerzat, and G. Cranston. 1995. “Mutations Derepressing Silent Centromeric Domains in Fission Yeast Disrupt Chromosome Segregation.” *Genes & Development* 9 (2): 218–33.

Alonso, Alicia, Dan Hasson, Fanny Cheung, and Peter E. Warburton. 2010. “A Paucity of Heterochromatin at Functional Human Neocentromeres.” *Epigenetics & Chromatin* 3 (1): 6.

Altemose, Nicolas, Karen H. Miga, Mauro Maggioni, and Huntington F. Willard. 2014. “Genomic Characterization of Large Heterochromatic Gaps in the Human Genome Assembly.” *PLoS Computational Biology* 10 (5): e1003628.

Ayoub, N., I. Goldshmidt, and A. Cohen. 1999. “Position Effect Variegation at the Mating-Type Locus of Fission Yeast: A Cis-Acting Element Inhibits Covariegated Expression of Genes in the Silent and Expressed Domains.” *Genetics* 152 (2): 495–508.

Bass, H. W., O. Riera-Lizarazu, E. V. Ananiev, S. J. Bordoli, H. W. Rines, R. L. Phillips, J. W. Sedat, D. A. Agard, and W. Z. Cande. 2000. “Evidence for the Coincident Initiation of Homolog Pairing and Synapsis during the Telomere-Clustering (bouquet) Stage of Meiotic Prophase.” *Journal of Cell Science* 113 (Pt 6) (March): 1033–42.

Becker, Justin S., Dario Nicetto, and Kenneth S. Zaret. 2016. “H3K9me3-Dependent Heterochromatin: Barrier to Cell Fate Changes.” *Trends in Genetics: TIG* 32 (1): 29–41.

Benjamini, Yuval, and Terence P. Speed. 2012. “Summarizing and Correcting the GC Content Bias in High-Throughput Sequencing.” *Nucleic Acids Research* 40 (10): e72.

Benson, G. 1999. “Tandem Repeats Finder: A Program to Analyze DNA Sequences.” *Nucleic Acids Research* 27 (2): 573–80.

Brahmachary, Manisha, Audrey Guilmatre, Javier Quilez, Dan Hasson, Christelle Borel, Peter Warburton, and Andrew J. Sharp. 2014. “Digital Genotyping of Macrosatellites and Multicopy Genes Reveals Novel Biological Functions Associated with Copy Number Variation of Large Tandem Repeats.”

bioRxiv preprint doi: https://doi.org/10.1101/470054; this version posted November 18, 2018. The copyright holder for this preprint (which was not certified by peer review) is the author/funder, who has granted bioRxiv a license to display the preprint in perpetuity. It is made available under aCC-BY-NC-ND 4.0 International license.

PLoS Genetics 10 (6): e1004418.

Brutlag, D. L. 1980. "Molecular Arrangement and Evolution of Heterochromatic DNA." *Annual Review of Genetics* 14: 121–44.

Calderón, María del Carmen, María-Dolores Rey, Adoración Cabrera, and Pilar Prieto. 2014. "The Subtelomeric Region Is Important for Chromosome Recognition and Pairing during Meiosis." *Scientific Reports* 4 (October): 6488.

Cann, Howard M., Claudia de Toma, Lucien Cazes, Marie-Fernande Legrand, Valerie Morel, Laurence Piouffre, Julia Bodmer, et al. 2002. "A Human Genome Diversity Cell Line Panel." *Science* 296 (5566): 261–62.

Chaisson, Mark J. P., John Huddleston, Megan Y. Dennis, Peter H. Sudmant, Maika Malig, Fereydoun Hormozdiari, Francesca Antonacci, et al. 2015. "Resolving the Complexity of the Human Genome Using Single-Molecule Sequencing." *Nature* 517 (7536): 608–11.

Cooke, H. 1976. "Repeated Sequence Specific to Human Males." *Nature* 262 (5565): 182–86.

Eberle, Michael A., Epameinondas Fritzilas, Peter Krusche, Morten Källberg, Benjamin L. Moore, Mitchell A. Bekritsky, Zamin Iqbal, et al. 2017. "A Reference Data Set of 5.4 Million Phased Human Variants Validated by Genetic Inheritance from Sequencing a Three-Generation 17-Member Pedigree." *Genome Research* 27 (1): 157–64.

Ferree, Patrick M., and Daniel A. Barbash. 2009. "Species-Specific Heterochromatin Prevents Mitotic Chromosome Segregation to Cause Hybrid Lethality in Drosophila." *PLoS Biology* 7 (10): e1000234.

Flynn, Jullien M., Ian Caldas, Melania E. Cristescu, and Andrew G. Clark. 2017. "Selection Constrains High Rates of Tandem Repetitive DNA Mutation in Daphnia Pulex." *Genetics* 207 (2): 697–710.

Flynn, Jullien M., Sarah E. Lower, Daniel A. Barbash, and Andrew G. Clark. 2018. "Rates and Patterns of Mutation in Tandem Repetitive DNA in Six Independent Lineages of Chlamydomonas Reinhardtii." *Genome Biology and Evolution* 10 (7): 1673–86.

Gall, Joseph G., Edward H. Cohen, and Mary Lake Polan. 1971. "Repetitive DNA Sequences in Drosophila." *Chromosoma* 33 (3): 319–44.

Gläser, B., F. Grützner, U. Willmann, R. Stanyon, N. Arnold, K. Taylor, W. Rietschel, S. Zeitler, R. Toder, and W. Schempp. 1998. "Simian Y Chromosomes: Species-Specific Rearrangements of DAZ, RBM, and TSPY versus Contiguity of PAR and SRY." *Mammalian Genome: Official Journal of the International Mammalian Genome Society* 9 (3): 226–31.

Glazko, Galina V., and Masatoshi Nei. 2003. "Estimation of Divergence Times for Major Lineages of Primate Species." *Molecular Biology and Evolution* 20 (3): 424–34.

Goodman, Morris, Lawrence I. Grossman, and Derek E. Wildman. 2005. "Moving Primate Genomics beyond the Chimpanzee Genome." *Trends in Genetics: TIG* 21 (9): 511–17.

Gordon, David, John Huddleston, Mark J. P. Chaisson, Christopher M. Hill, Zev N. Kronenberg, Katherine M. Munson, Maika Malig, et al. 2016. "Long-Read Sequence Assembly of the Gorilla Genome." *Science* 352 (6281): aae0344.

Gowen, J. W., and E. H. Gay. 1933. "EFFECT OF TEMPERATURE ON EVERSPORTING EYE COLOR IN DROSOPHILA MELANOGASTER." *Science* 77 (1995): 312.

Grady, D. L., R. L. Ratliff, D. L. Robinson, E. C. McCanlies, J. Meyne, and R. K. Moyzis. 1992. "Highly Conserved Repetitive DNA Sequences Are Present at Human Centromeres." *Proceedings of the National Academy of Sciences of the United States of America* 89 (5): 1695–99.

Grenier, J. K., J. R. Arguello, M. C. Moreira, S. Gottipati, J. Mohammed, S. R. Hackett, and Others. n.d. "Global Diversity Lines--A Five-Continent Reference Panel of Sequenced Drosophila Melanogaster Strains. G3: Genes| Genomes| Genetics. 2015; 5 (4): 593--603."

Gudbjartsson, Daniel F., Hannes Helgason, Sigurjon A. Gudjonsson, Florian Zink, Asmundur Oddson, Arnaldur Gylfason, Soren Besenbacher, et al. 2015. "Large-Scale Whole-Genome Sequencing of the Icelandic Population." *Nature Genetics* 47 (5): 435–44.

Hallast, Pille, Pierpaolo Maisano Delser, Chiara Batini, Daniel Zadik, Mariano Rocchi, Werner Schempp, Chris Tyler-Smith, and Mark A. Jobling. 2016. "Great Ape Y Chromosome and Mitochondrial DNA Phylogenies Reflect Subspecies Structure and Patterns of Mating and Dispersal." *Genome Research* 26 (4): 427–39.

Harris S. B., Cechova M., Makova D. K., "Noise-Cancelling Repeat Finder: Uncovering tandem repeats in error-prone long-read sequencing data". *Bioinformatics* (submitted).

Hayden, Karen E., Erin D. Strome, Stephanie L. Merrett, Hye-Ran Lee, M. Katharine Rudd, and Huntington F. Willard. 2013. "Sequences Associated with Centromere Competency in the Human

bioRxiv preprint doi: https://doi.org/10.1101/470054; this version posted November 18, 2018. The copyright holder for this preprint (which was not certified by peer review) is the author/funder, who has granted bioRxiv a license to display the preprint in perpetuity. It is made available under aCC-BY-NC-ND 4.0 International license.

Genome." *Molecular and Cellular Biology* 33 (4): 763–72.
Heitz, E. 1928. "Das Heterochromatin Der Moose. Jb. Bot. 69: 762-818. 1932 Die Herkunft Der Chromocentren." *Planta*.
Helleu, Quentin, Pierre R. Gérard, Raphaëlle Dubruille, David Ogereau, Benjamin Prud'homme, Benjamin Loppin, and Catherine Montchamp-Moreau. 2016. "Rapid Evolution of a Y-Chromosome Heterochromatin Protein Underlies Sex Chromosome Meiotic Drive." *Proceedings of the National Academy of Sciences of the United States of America* 113 (15): 4110–15.
Howe, Bradley, Ayesha Umrigar, and Fern Tsien. 2014. "Chromosome Preparation from Cultured Cells." *Journal of Visualized Experiments: JoVE*, no. 83 (January): e50203.
Hughes, Jennifer F., and Steve Rozen. 2012. "Genomics and Genetics of Human and Primate Y Chromosomes." *Annual Review of Genomics and Human Genetics* 13 (April): 83–108.
Hughes, Jennifer F., Helen Skaletsky, Tatyana Pyntikova, Tina A. Graves, Saskia K. M. van Daalen, Patrick J. Minx, Robert S. Fulton, et al. 2010. "Chimpanzee and Human Y Chromosomes Are Remarkably Divergent in Structure and Gene Content." *Nature* 463 (7280): 536–39.
Ip, Camilla L. C., Matthew Loose, John R. Tyson, Mariateresa de Cesare, Bonnie L. Brown, Miten Jain, Richard M. Leggett, et al. 2015. "MinION Analysis and Reference Consortium: Phase 1 Data Release and Analysis." *F1000Research* 4 (October): 1075.
Jain, Miten, Sergey Koren, Karen H. Miga, Josh Quick, Arthur C. Rand, Thomas A. Sasani, John R. Tyson, et al. 2018. "Nanopore Sequencing and Assembly of a Human Genome with Ultra-Long Reads." *Nature Biotechnology* 36 (4): 338–45.
Jain, Miten, Hugh E. Olsen, Daniel J. Turner, David Stoddart, Kira V. Bulazel, Benedict Paten, David Haussler, Huntington F. Willard, Mark Akeson, and Karen H. Miga. 2018. "Linear Assembly of a Human Centromere on the Y Chromosome." *Nature Biotechnology* 36 (4): 321–23.
Jarmuż, Malgorzata, Caron D. Glotzbach, Kristen A. Bailey, Ruma Bandyopadhyay, and Lisa G. Shaffer. 2007. "The Evolution of Satellite III DNA Subfamilies among Primates." *American Journal of Human Genetics* 80 (3): 495–501.
Jolly, Caroline, Alexandra Metz, Jérôme Govin, Marc Vigneron, Bryan M. Turner, Saadi Khochbin, and Claire Vourc'h. 2004. "Stress-Induced Transcription of Satellite III Repeats." *The Journal of Cell Biology* 164 (1): 25–33.
Kelsey, Keegan J. P., and Andrew G. Clark. 2017. "Variation in Position Effect Variegation Within a Natural Population." *Genetics* 207 (3): 1157–66.
Kit, S. 1961. "Equilibrium Sedimentation in Density Gradients of DNA Preparations from Animal Tissues." *Journal of Molecular Biology* 3 (December): 711–16.
Koga, Akihiko, Morihiro Notohara, and Hirohisa Hirai. 2011. "Evolution of Subterminal Satellite (StSat) Repeats in Hominids." *Genetica* 139 (2): 167–75.
Krishan, Awtar, Payal Dandekar, Nirmal Nathan, Ronald Hamelik, Christine Miller, and Jackie Shaw. 2005. "DNA Index, Genome Size, and Electronic Nuclear Volume of Vertebrates from the Miami Metro Zoo." *Cytometry. Part A: The Journal of the International Society for Analytical Cytology* 65 (1): 26–34.
Kronenberg, Zev N., Ian T. Fiddes, David Gordon, Shwetha Murali, Stuart Cantsilieris, Olivia S. Meyerson, Jason G. Underwood, et al. 2018. "High-Resolution Comparative Analysis of Great Ape Genomes." *Science* 360 (6393). https://doi.org/10.1126/science.aar6343.
Kunkel, L. M., K. D. Smith, and S. H. Boyer. 1976. "Human Y-Chromosome-Specific Reiterated DNA." *Science* 191 (4232): 1189–90.
Lemos, Bernardo, Luciana O. Araripe, and Daniel L. Hartl. 2008. "Polymorphic Y Chromosomes Harbor Cryptic Variation with Manifold Functional Consequences." *Science* 319 (5859): 91–93.
Lemos, Bernardo, Alan T. Branco, and Daniel L. Hartl. 2010. "Epigenetic Effects of Polymorphic Y Chromosomes Modulate Chromatin Components, Immune Response, and Sexual Conflict." *Proceedings of the National Academy of Sciences of the United States of America* 107 (36): 15826–31.
Lieberman-Aiden, Erez, Nynke L. van Berkum, Louise Williams, Maxim Imakaev, Tobias Ragoczy, Agnes Telling, Ido Amit, et al. 2009. "Comprehensive Mapping of Long-Range Interactions Reveals Folding Principles of the Human Genome." *Science* 326 (5950): 289–93.
Lohe, A. R., and D. L. Brutlag. 1987. "Identical Satellite DNA Sequences in Sibling Species of Drosophila." *Journal of Molecular Biology* 194 (2): 161–70.
Lower, Sarah Sander, Michael P. McGurk, Andrew G. Clark, and Daniel A. Barbash. 2018. "Satellite DNA

bioRxiv preprint doi: https://doi.org/10.1101/470054; this version posted November 18, 2018. The copyright holder for this preprint (which was not certified by peer review) is the author/funder, who has granted bioRxiv a license to display the preprint in perpetuity. It is made available under aCC-BY-NC-ND 4.0 International license.

Evolution: Old Ideas, New Approaches." *Current Opinion in Genetics & Development* 49 (April): 70–78.

Lu, Hengyun, Francesca Giordano, and Zemin Ning. 2016. "Nanopore MinION Sequencing and Genome Assembly." *Genomics, Proteomics & Bioinformatics* 14 (5): 265–79.

Manfredi-Romanini, M. G. 1972. "Nuclear DNA Content and Area of Primate Lymphocytes as a Cytotaxonomical Tool." *Journal of Human Evolution* 1 (1): 23–40.

Manuelidis, L. 1978. "Chromosomal Localization of Complex and Simple Repeated Human DNAs." *Chromosoma* 66 (1): 23–32.

Meiklejohn, Colin D. 2016. "Heterochromatin and Genetic Conflict." *Proceedings of the National Academy of Sciences of the United States of America* 113 (15): 3915–17.

Melters, Daniël P., Keith R. Bradnam, Hugh A. Young, Natalie Telis, Michael R. May, J. Graham Ruby, Robert Sebra, et al. 2013. "Comparative Analysis of Tandem Repeats from Hundreds of Species Reveals Unique Insights into Centromere Evolution." *Genome Biology* 14 (1): R10.

Meyer, Matthias, Martin Kircher, Marie-Theres Gansauge, Heng Li, Fernando Racimo, Swapan Mallick, Joshua G. Schraiber, et al. 2012. "A High-Coverage Genome Sequence from an Archaic Denisovan Individual." *Science* 338 (6104): 222–26.

Miga, Karen H., Yulia Newton, Miten Jain, Nicolas Altemose, Huntington F. Willard, and W. James Kent. 2014. "Centromere Reference Models for Human Chromosomes X and Y Satellite Arrays." *Genome Research* 24 (4): 697–707.

Nakahori, Y., K. Mitani, M. Yamada, and Y. Nakagome. 1986. "A Human Y-Chromosome Specific Repeated DNA Family (DYZ1) Consists of a Tandem Array of Pentanucleotides." *Nucleic Acids Research* 14 (19): 7569–80.

Novo, Clara, Nausica Arnoult, Win-Yan Bordes, Luis Castro-Vega, Anne Gibaud, Bernard Dutrillaux, Silvia Bacchetti, and Arturo Londoño-Vallejo. 2013. "The Heterochromatic Chromosome Caps in Great Apes Impact Telomere Metabolism." *Nucleic Acids Research* 41 (9): 4792–4801.

Pellicciari, C., E. Ronchetti, R. Tori, D. Formenti, and M. G. Manfredi Romanini. 1990. "Cytochemical Evaluation of C-Heterochromatic-DNA in Metaphase Chromosomes." *Basic and Applied Histochemistry* 34 (1): 79–85.

Plohl, Miroslav, Andrea Luchetti, Nevenka Mestrović, and Barbara Mantovani. 2008. "Satellite DNAs between Selfishness and Functionality: Structure, Genomics and Evolution of Tandem Repeats in Centromeric (hetero)chromatin." *Gene* 409 (1-2): 72–82.

Prado-Martinez, Javier, Peter H. Sudmant, Jeffrey M. Kidd, Heng Li, Joanna L. Kelley, Belen Lorente-Galdos, Krishna R. Veeramah, et al. 2013. "Great Ape Genetic Diversity and Population History." *Nature* 499 (7459): 471–75.

Quilez, Javier, Audrey Guilmatre, Paras Garg, Gareth Highnam, Melissa Gymrek, Yaniv Erlich, Ricky S. Joshi, David Mittelman, and Andrew J. Sharp. 2016. "Polymorphic Tandem Repeats within Gene Promoters Act as Modifiers of Gene Expression and DNA Methylation in Humans." *Nucleic Acids Research* 44 (8): 3750–62.

Rhoads, Anthony, and Kin Fai Au. 2015. "PacBio Sequencing and Its Applications." *Genomics, Proteomics & Bioinformatics* 13 (5): 278–89.

Rosenberg, Noah A., Jonathan K. Pritchard, James L. Weber, Howard M. Cann, Kenneth K. Kidd, Lev A. Zhivotovsky, and Marcus W. Feldman. 2002. "Genetic Structure of Human Populations." *Science* 298 (5602): 2381–85.

Rošić, Silvana, Florian Köhler, and Sylvia Erhardt. 2014. "Repetitive Centromeric Satellite RNA Is Essential for Kinetochore Formation and Cell Division." *The Journal of Cell Biology* 207 (3): 335–49.

Royle, N. J., D. M. Baird, and A. J. Jeffreys. 1994. "A Subterminal Satellite Located Adjacent to Telomeres in Chimpanzees Is Absent from the Human Genome." *Nature Genetics* 6 (1): 52–56.

Skaletsky, Helen, Tomoko Kuroda-Kawaguchi, Patrick J. Minx, Holland S. Cordum, Ladeana Hillier, Laura G. Brown, Sjoerd Repping, et al. 2003. "The Male-Specific Region of the Human Y Chromosome Is a Mosaic of Discrete Sequence Classes." *Nature* 423 (6942): 825–37.

Solovei, Irina, Moritz Kreysing, Christian Lanctôt, Süleyman Kösem, Leo Peichl, Thomas Cremer, Jochen Guck, and Boris Joffe. 2009. "Nuclear Architecture of Rod Photoreceptor Cells Adapts to Vision in Mammalian Evolution." *Cell* 137 (2): 356–68.

Soufi, Abdenour, Greg Donahue, and Kenneth S. Zaret. 2012. "Facilitators and Impediments of the Pluripotency Reprogramming Factors' Initial Engagement with the Genome." *Cell* 151 (5): 994–1004.

Spinelli, Gino. 2003. "Heterochromatin and Complexity: A Theoretical Approach." *Nonlinear Dynamics,*

bioRxiv preprint doi: https://doi.org/10.1101/470054; this version posted November 18, 2018. The copyright holder for this preprint (which was not certified by peer review) is the author/funder, who has granted bioRxiv a license to display the preprint in perpetuity. It is made available under aCC-BY-NC-ND 4.0 International license.

Psychology, and Life Sciences 7 (4): 329–61.

Spofford, J. B. 1976. "Position-Effect Variegation in Drosophila." *The Genetics and Biology of Drosophila*.

Stephens, Zachary D., and Ravishankar K. Iyer. 2018. "Measuring the Mappability Spectrum of Reference Genome Assemblies." In *Proceedings of the 2018 ACM International Conference on Bioinformatics, Computational Biology, and Health Informatics*, 47–52. BCB '18. New York, NY, USA: ACM.

Subramanian, Subbaya, Rakesh K. Mishra, and Lalji Singh. 2003. "Genome-Wide Analysis of Microsatellite Repeats in Humans: Their Abundance and Density in Specific Genomic Regions." *Genome Biology* 4 (2): R13.

Sueoka, Noboru. 1961. "Variation and Heterogeneity of Base Composition of Deoxyribonucleic Acids: A Compilation of Old and New Data." *Journal of Molecular Biology* 3 (1): 31–IN15.

Sujiwattanarat, Penporn, Watcharaporn Thapana, Kornsorn Srikulnath, Yuriko Hirai, Hirohisa Hirai, and Akihiko Koga. 2015. "Higher-Order Repeat Structure in Alpha Satellite DNA Occurs in New World Monkeys and Is Not Confined to Hominoids." *Scientific Reports* 5 (May): 10315.

Surabhi, Surabhi, Akshay Kumar Avvaru, Divya Tej Sowpati, and Rakesh K. Mishra. 2018. "Patterns of Microsatellite Distribution Reflect the Evolution of Biological Complexity." *bioRxiv*. https://doi.org/10.1101/253930.

Tagarro, I., A. M. Fernández-Peralta, and J. J. González-Aguilera. 1994. "Chromosomal Localization of Human Satellites 2 and 3 by a FISH Method Using Oligonucleotides as Probes." *Human Genetics* 93 (4): 383–88.

Tamura, Koichiro, Sankar Subramanian, and Sudhir Kumar. 2004. "Temporal Patterns of Fruit Fly (Drosophila) Evolution Revealed by Mutation Clocks." *Molecular Biology and Evolution* 21 (1): 36–44.

Tomaszkiewicz, Marta, Samarth Rangavittal, Monika Cechova, Rebeca Campos Sanchez, Howard W. Fescemyer, Robert Harris, Danling Ye, et al. 2016. "A Time- and Cost-Effective Strategy to Sequence Mammalian Y Chromosomes: An Application to the de Novo Assembly of Gorilla Y." *Genome Research* 26 (4): 530–40.

Ventura, Mario, Claudia R. Catacchio, Saba Sajjadian, Laura Vives, Peter H. Sudmant, Tomas Marques-Bonet, Tina A. Graves, Richard K. Wilson, and Evan E. Eichler. 2012. "The Evolution of African Great Ape Subtelomeric Heterochromatin and the Fusion of Human Chromosome 2." *Genome Research* 22 (6): 1036–49.

Vinogradov, A. E. 1998. "Genome Size and GC□percent in Vertebrates as Determined by Flow Cytometry: The Triangular Relationship." *Cytometry. Part A: The Journal of the International Society for Analytical Cytology*. http://onlinelibrary.wiley.com/doi/10.1002/(SICI)1097-0320(19980201)31:2%3C100::AID-CYTO5%3E3.0.CO;2-Q/full.

Walker, P. M. 1971. "Origin of Satellite DNA." *Nature* 229 (5283): 306–8.

Wei, Kevin H-C, Jennifer K. Grenier, Daniel A. Barbash, and Andrew G. Clark. 2014. "Correlated Variation and Population Differentiation in Satellite DNA Abundance among Lines of Drosophila Melanogaster." *Proceedings of the National Academy of Sciences* 111 (52): 18793–98.

Wei, Kevin H-C, Sarah E. Lower, Ian V. Caldas, Trevor J. S. Sless, Daniel A. Barbash, and Andrew G. Clark. 2018. "Variable Rates of Simple Satellite Gains across the Drosophila Phylogeny." *Molecular Biology and Evolution* 35 (4): 925–41.

Wolfe, J., S. M. Darling, R. P. Erickson, I. W. Craig, V. J. Buckle, P. W. Rigby, H. F. Willard, and P. N. Goodfellow. 1985. "Isolation and Characterization of an Alphoid Centromeric Repeat Family from the Human Y Chromosome." *Journal of Molecular Biology* 182 (4): 477–85.

Yang, Fengtang, Vladimir Trifonov, Bee Ling Ng, Nadezda Kosyakova, and Nigel P. Carter. 2009. "Generation of Paint Probes by Flow-Sorted and Microdissected Chromosomes." In *Fluorescence In Situ Hybridization (FISH) — Application Guide*, edited by Thomas Liehr, 35–52. Berlin, Heidelberg: Springer Berlin Heidelberg.

Yunis, Jorge J., and Walid G. Yasmineh. 1971. "Heterochromatin, Satellite DNA, and Cell Function." *Science* 174 (4015): 1200–1209.

Zhang, Weiqi, Jingyi Li, Keiichiro Suzuki, Jing Qu, Ping Wang, Junzhi Zhou, Xiaomeng Liu, et al. 2015. "A Werner Syndrome Stem Cell Model Unveils Heterochromatin Alterations as a Driver of Human Aging." *Science* 348 (6239): 1160–63.

Zhou, Qi, and Doris Bachtrog. 2015. "Ancestral Chromatin Configuration Constrains Chromatin Evolution on Differentiating Sex Chromosomes in Drosophila." *PLoS Genetics* 11 (6): e1005331.

bioRxiv preprint doi: https://doi.org/10.1101/470054; this version posted November 18, 2018. The copyright holder for this preprint (which was not certified by peer review) is the author/funder, who has granted bioRxiv a license to display the preprint in perpetuity. It is made available under aCC-BY-NC-ND 4.0 International license.

Zook, Justin M., David Catoe, Jennifer McDaniel, Lindsay Vang, Noah Spies, Arend Sidow, Ziming Weng, et al. 2015. "Extensive Sequencing of Seven Human Genomes to Characterize Benchmark Reference Materials." *bioRxiv*. https://doi.org/10.1101/026468.

———. 2016. "Extensive Sequencing of Seven Human Genomes to Characterize Benchmark Reference Materials." *Scientific Data* 3 (June): 160025.

Figure legends

Figure 1. Densities and similarity among satellite repeats in great apes. (A) Intra- and interspecific variation in overall repeat density. Repeat densities are plotted for each species and subspecies. Each dot represents a single individual, and bars are mean values. For species comprising subspecies, a species-level average is also represented as a bar. Human (N=9, black), bonobo (N=13, blue), chimpanzee (N=19, green), gorilla (N=27, red), S. orangutan is Sumatran orangutan (N=5, yellow), and B. orangutan is Bornean orangutan (N=5, orange). The cross river gorilla has sample size of 1 and is only included in the species-level analysis. **(B) Heatmap of average repeat densities (across individuals) for the 39 abundant repeats in each of the six species.** Color coding from dark to light blue represents high to low values. Repeats present at less than 100 loci per 20 million reads are considered absent (white cells). $(AATGG)_n$-derived and 32-mer-derived repeated motifs are separated by a horizontal line. Cumulative densities of abundant repeats and of all repeats are calculated as averages across all individuals. **(C) Similarity and inter-relatedness among the sequences of 39 abundant repeated motifs.** Each circle represents a repeat (indexes inside the circles match those in Fig. 1B). The sizes of circles represent four categories of repeat densities from smallest to largest: 0-0.1 kb/Mb, 0.1-1 kb/Mb, 1-10 kb/Mb, and >10 kb/Mb. The color of a link represents the number of substitutions (see Methods) needed for the shorter repeated motif to perfectly match the longer related repeated motif (yellow: one step; orange: two steps; red: three steps). The circles depicting repeated motifs related to 32-mers are filled in green; the ones corresponding to all other repeated motifs (usually related to $(AATGG)_n$) are filled in yellow.

Figure 2. Relatedness of 88 analyzed individuals belonging to six great ape species. (A) Principal Component Analysis. Individuals are plotted as circles in the space of the first three principal components extracted from the densities of the 39 abundant repeats, which explain 98% of the variance. Colors correspond to the six species: human (black), bonobo (blue), chimpanzee (green), gorilla (red), Sumatran orangutan (orange), and Bornean orangutan (gold). **(B) Cross-validation accuracy of a Linear Discriminant Analysis classification of individuals into species, as a function of the number of abundant repeats used.** The 39 abundant repeats were progressively added to the LDA classifier in decreasing order of abundance. Using the motif indexes from Fig. 1B, this order was: 1, 30, 17, 24, 11, 22, 29, 10, 20, 36, 25, 12, 3, 26, 13, 15, 34, 32, 39, 2, 35, 4, 18, 33, 9, 16, 23, 19, 37, 5, 8, 21, 27, 28, 31, 6, 7, 14, and 38. The accuracy increases as the first 20 repeated motifs are added, and then decreases due to overfitting. The blue vertical line marks the first 14 repeated motifs, and the red horizontal one the 95% accuracy level. **(C) Hierarchical clustering of individuals.** This clustering employs the densities of all 5,494 repeated motifs, Spearman correlations, and complete linkage. **(D) Species topology based on repeats presence/absence.** A schematic figure showing repeated motifs unique to a species (terminal branches) and those that are shared among the species descending from internal branches. On the left, the tree is built based on the presence/absence of repeated motifs, iteratively joining species sharing the most repeated motifs. On the right, the tree is built according to the accepted species phylogeny (Goodman et al. 2005) and the number of shared repeated motifs is indicated. The branch widths are

bioRxiv preprint doi: https://doi.org/10.1101/470054; this version posted November 18, 2018. The copyright holder for this preprint (which was not certified by peer review) is the author/funder, who has granted bioRxiv a license to display the preprint in perpetuity. It is made available under aCC-BY-NC-ND 4.0 International license.

proportional to the number of repeated motifs (branch lengths are uninformative). 83 repeated motifs (the number shown in the middle) were shared among all six studied species.

Figure 3. Spearman correlations for the densities of the 39 abundant repeats in human and gorilla. Colored dots in the upper (**A**; Human, n=105 comparisons) and lower (**C**; Gorilla, n=528 comparisons) left panels show observed correlations between pairs of repeats plotted in non-decreasing order, in red when positive and in blue when negative. Chance background correlations, again in non-decreasing order, are plotted in black with variation bands in gray (see Methods). The heatmaps in the upper (**B**; Human) and lower (**D**; Gorilla) right panels show the correlations corresponding to each repeat pair, with various intensities of red (positive) and blue (negative). The size of the circles is also proportional to that of the correlation. Fig. S9 provides the same information for the other species. Only repeats present in the relevant species are shown.

Figure 4. Fluorescent in situ hybridization (FISH) analysis. Hybridization of: **(A)** the 5'-amine-modified probe Pan32 (with a candidate 32-mer male-biased motif sequence) to DAPI-counterstained chimpanzee male chromosomes; **(B)** the 5'-amine-modified probe Pan32 to DAPI-counterstained bonobo male chromosomes; **(C)** the whole bonobo Y chromosome painting probe (WBY) to DAPI-counterstained bonobo male chromosomes; and **(D)** both the WBY and Pan32 probes. The arrow indicates the location of the bonobo Y chromosome. The 5'-amine-modified probe Pan32 is labeled with Alexa Fluor (green). The WBY probe is labeled with digoxigenin. Scale bar = 10 um.

Figure 5. Analysis of repeat density in three human trios. (A) Repeat densities from trio data (repeated motifs absent in human are not shown). **(B)** From left to right: two trios (77 and 78) with CEU ancestry are shown first, followed by the Ashkenazi trio (HG). The repeat density for the $(AATGG)_n$ repeat (in gray) and other repeats (in color). **(C)** Inter-generational change in repeat density. The vertical line represents repeat density in a child. The difference in repeat density between a child and a parent is marked in blue (father) or red (mother).

Figure 6. Repeat densities inferred from long sequencing reads generated with Nanopore (in-house) and PacBio (from public datasets) technologies. The whole-genome PacBio data for bonobo and Bornean orangutan are not available**.**

Figure 7. Box plots of lengths of (A) reads, (B) repeated motif $(AATGG)_n$, and (C) one 32-mer recovered, from Nanopore data.

Figure 1

A

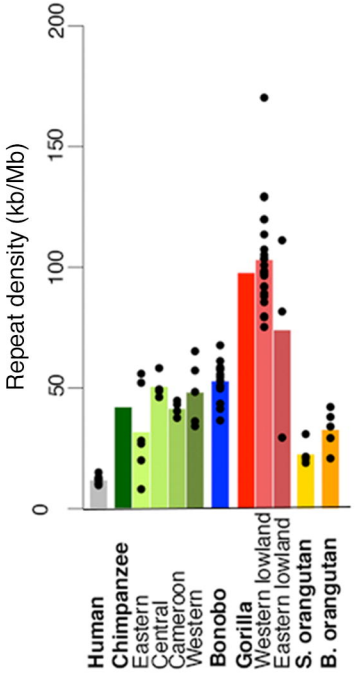

B

	Gorilla (N=27)	Chimpanzee (N=19)	Bonobo (N=13)	Human (N=9)	S. orangutan (N=5)	B. orangutan (N=5)
(1) AATGG	22.12	5.53	13.96	6.63	10.18	14.64
(2) ACTCC	0.05	0.04	0.03	0.13	0.61	0.75
(3) AAAG	0.17	0.28	0.21	0.18	0.18	0.18
(4) AATGGAGTGG	0.02	0.02	0.01	0.05	0.33	0.41
(5) AATGGAATGGAGTGG	0.01	0.01	0.01	0.03	0.12	0.16
(6) AATGGAGTGGAGTGG	0.01	0.01	0.01	0.02	0.12	0.15
(7) AAGTGGAATGG	<0.01				0.11	0.17
(8) AATGGAATGTG					0.12	0.17
(9) AAAGTGGAATGG					0.27	0.4
(10) AACGTGGAATGG		<0.01			0.81	1.27
(11) AATGGAATGTGG	<0.01	0.01			5.47	8.39
(12) AATGGAATGGAATGTGG		<0.01			0.64	0.93
(13) AATGGAATGGAATGGAATGTGG		<0.01			0.62	0.88
(14) AAATGGACTCGAATGGAATCATC	<0.01	<0.01	<0.01	0.08		
(15) AATCGAATGGAATGG	0.01	0.01	0.02	0.14		
(16) AAATGGAATCGAATGGAATCATC	<0.01	<0.01	<0.01	0.12		
(17) AATCATCGAATGGAATCGAATGG	<0.01	<0.01	0.01	0.38		
(18) AATCATCGAATGGACTCGAATGG	<0.01	<0.01	<0.01	0.13		
(19) AATCATCATGAATGGAATCGAATGG	<0.01	<0.01	<0.01	0.08		
(20) AAATGGAATCGAATGGAATCATCATC	<0.01	<0.01	<0.01	0.25		
(21) AAATGGAATCGAATGTAATCATCATC				0.08		
(22) AATCATCATCGAATGGAATCGAATGG	0.01	0.01	0.01	0.26		
(23) AAACATGTAAATATTTACACAGAATCTGTAT	0.01	0.45	0.55			
(24) AAATATCTACACCGCTATCTGTATGAACATGG	16.78	0.01	0.04			0.02
(25) AAATATCTACACCGCCATCTGTATGAACATGG	6.37	0.01	0.01			0.01
(26) AAACATGGAAATATCTACACAGCCATCTGTAT	0.08	1.53	1.23		<0.01	
(27) AAACATGGAAATATCTACACCACCATCTGTAT	0.13	0.37	0.45			
(28) AAACATGGAAATATCTACACCACTATCTGTAT	0.22	0.33	0.48			
(29) AAACATGGAAATATCTACACCGCCATCTGTAT	1.5	1.99	1.99		<0.01	<0.01
(30) AAACATGGAAATATCTACACCGCTATCTGTAT	8.88	6.1	6.32		0.01	0.02
(31) AAACATGGAAATATCTACACCGCTATCTGTGT	0.71	0.21	0.3			
(32) AAACATGGAAATATCTACACTGCCATCTGTAT	0.1	0.75	0.81		<0.01	
(33) AAACATGGAAATATCTACACTGCTATCTGTAT	0.81	0.54	0.54			
(34) AAACATGGAAATATCTACACCGCGATCTGTAT	0.01	1.18	0.8		<0.01	
(35) AAACATGGAAATATCTACACCGCCATCTCTAT	0.75	0.78	0.68			
(36) AAACATGGAAATATCTACACCGCTATCTCTAT	0.91	1.57	1.55		<0.01	
(37) AAATATCTACACAGCTATCTGTATGAACATGG	0.74	<0.01	0.01			
(38) AAATATCTACACCACTATCTGTATGAACATGG	0.66		0.01			
(39) AAATATCTACACCGCTATCTGCATGAACATGG	0.94		0.01			
Cumulative density of abundant repeats	92.28	37.98	43.41	8.63	18.40	27.12
Cumulative density of all repeats	97.76	42.16	52.93	11.89	22.65	32.84

C

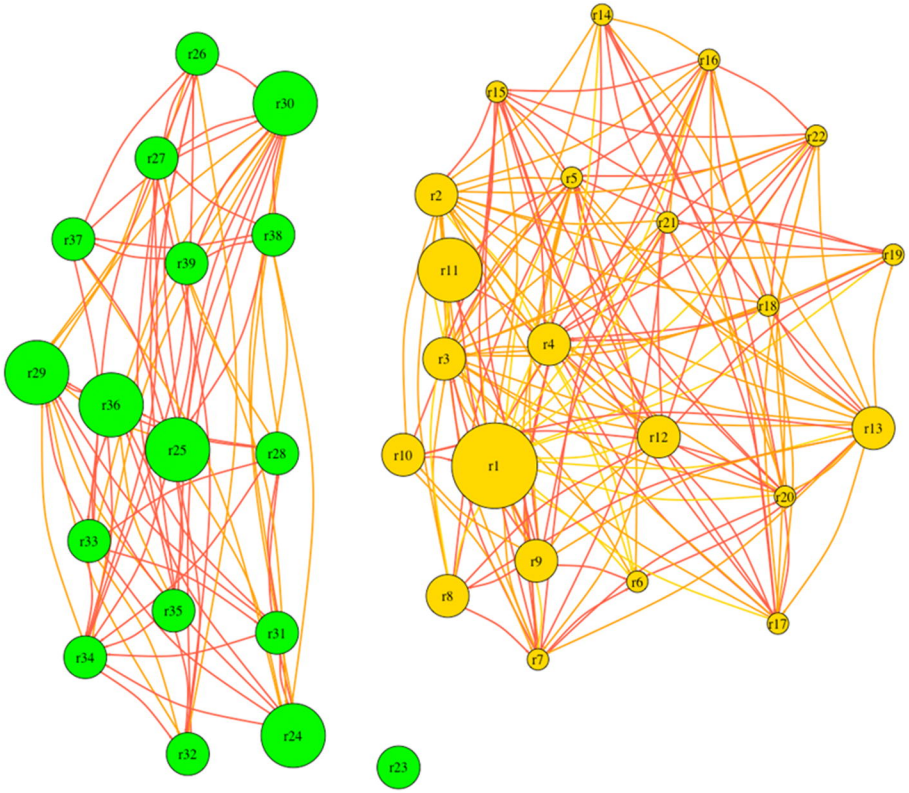

Figure 2

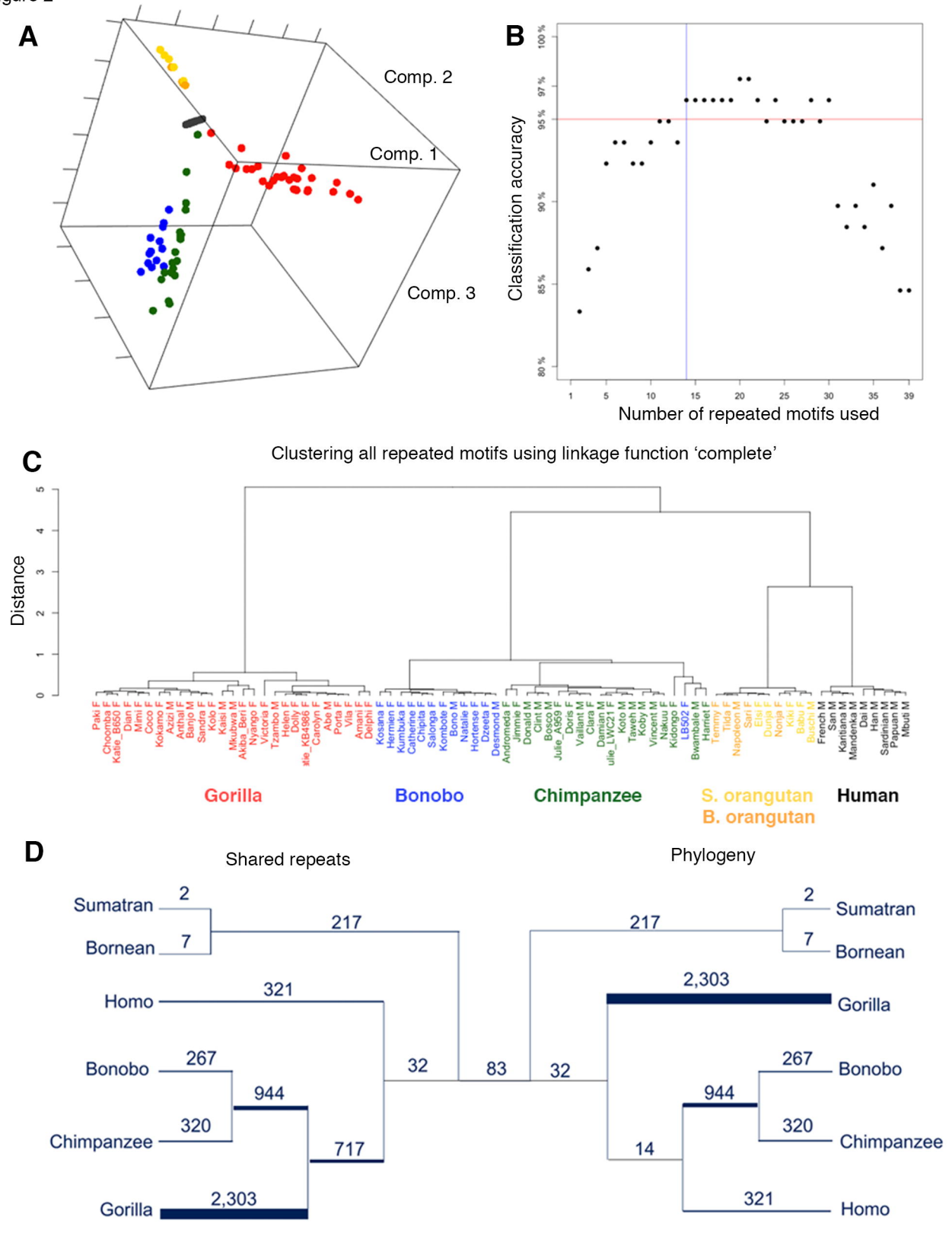
A
Comp. 2
Comp. 1
Comp. 3
B
Classification accuracy
Number of repeated motifs used
C
Clustering all repeated motifs using linkage function 'complete'
Distance
Gorilla
Bonobo
Chimpanzee
S. orangutan
B. orangutan
Human
D
Shared repeats
Phylogeny
Sumatran
Bornean
Homo
Bonobo
Chimpanzee
Gorilla
2
7
217
321
267
944
320
717
2,303
32
83
32
14
2,303
267
944
320
321

Figure 3

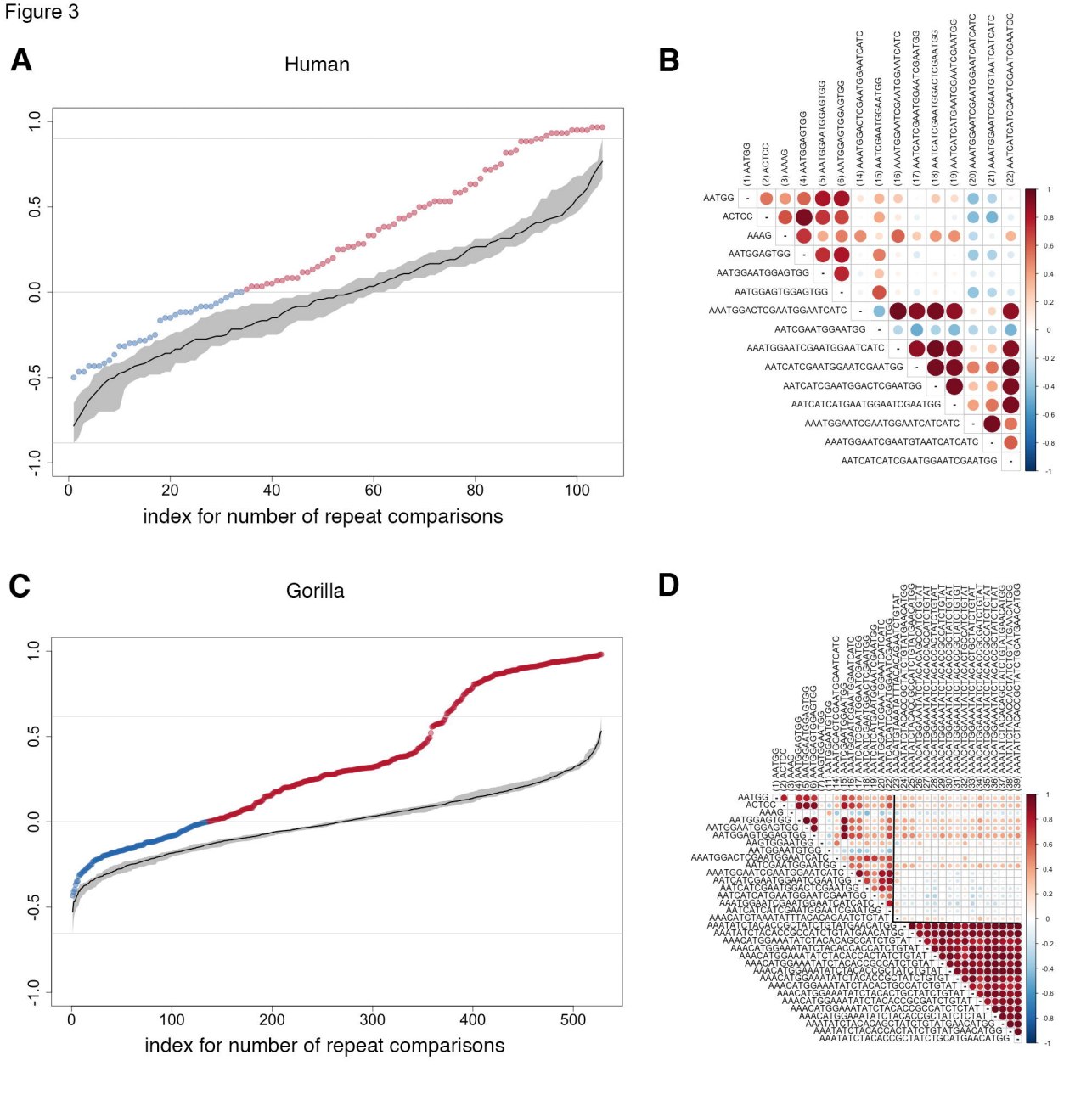
A
Human
index for number of repeat comparisons
B
C
Gorilla
index for number of repeat comparisons
D

Figure 4

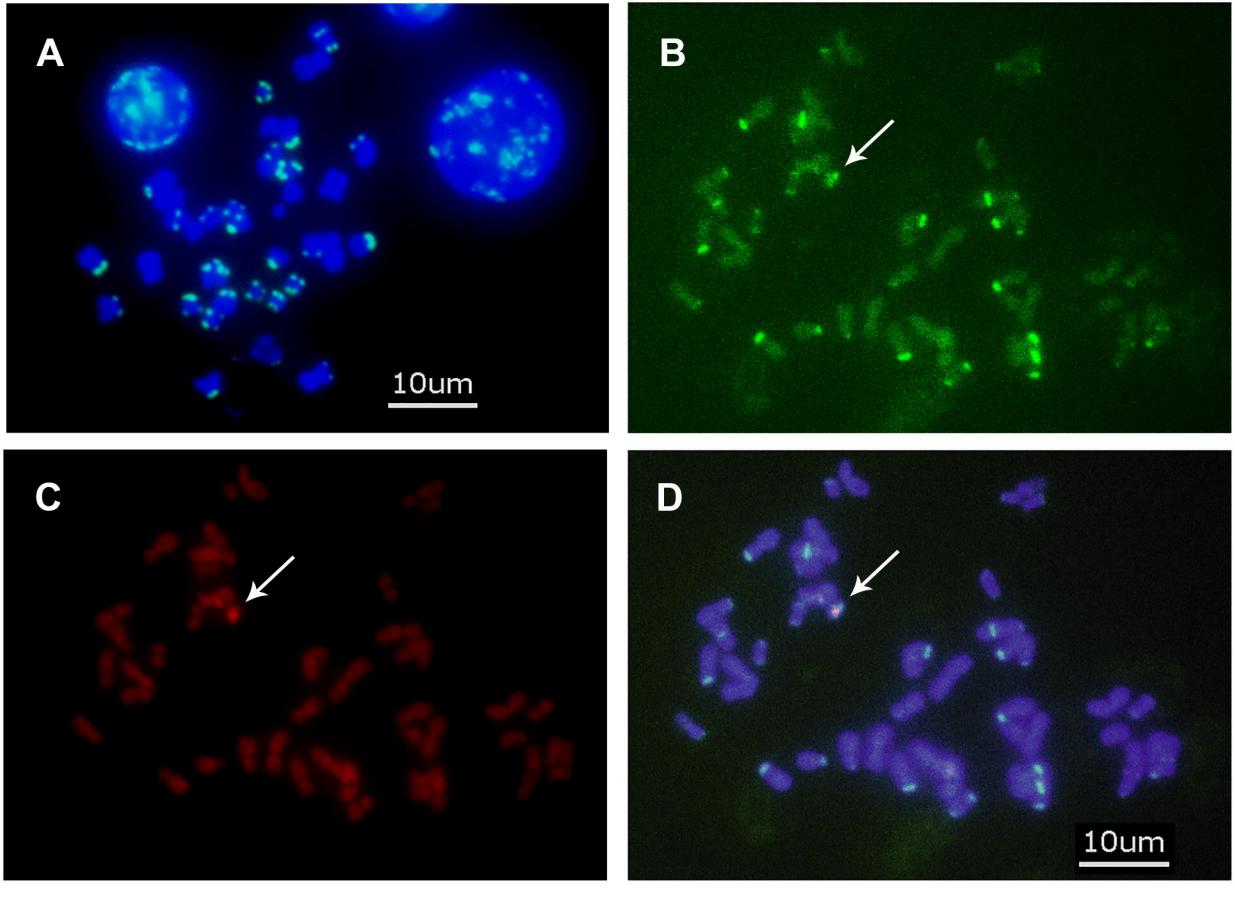

Figure 5

A

	Father 77	Father 78	Father HG	Son 77	Son HG	Mother 77	Mother 78	Mother HG	Daughter 78
(1) AATGG	4.22	4.21	6.1	4.21	5.76	3.36	3.7	5.17	3.71
(2) ACTCC	0.08	0.09	0.12	0.09	0.11	0.06	0.08	0.11	0.09
(3) AAAG	0.17	0.18	0.18	0.17	0.19	0.17	0.19	0.19	0.2
(4) AATGGAGTGG	0.03	0.04	0.05	0.04	0.05	0.03	0.03	0.05	0.04
(5) AATGGAATGGAGTGG	0.02	0.02	0.03	0.02	0.02	0.01	0.02	0.02	0.02
(6) AATGGAGTGGAGTGG	0.01	0.01	0.02	0.01	0.02	0.01	0.01	0.02	0.01
(14) AAATGGACTCGAATGGAATCATC	0.06	0.07	0.1	0.05	0.06	0.03	0.03	0.05	0.06
(15) AATCGAATGGAATGG	0.11	0.12	0.18	0.1	0.17	0.03	0.05	0.07	0.06
(16) AAATGGAATCGAATGGAATCATC	0.09	0.1	0.14	0.08	0.09	0.05	0.05	0.08	0.08
(17) AATCATCGAATGGAATCGAATGG	0.27	0.36	0.48	0.25	0.35	0.23	0.27	0.34	0.3
(18) AATCATCGAATGGACTCGAATGG	0.11	0.14	0.18	0.1	0.12	0.07	0.08	0.11	0.11
(19) AATCATCATGAATGGAATCGAATGG	0.05	0.06	0.08	0.05	0.06	0.04	0.05	0.06	0.05
(20) AAATGGAATCGAATGGAATCATCATC	0.16	0.21	0.26	0.16	0.21	0.19	0.21	0.22	0.19
(21) AAATGGAATCGAATGTAATCATCATC	0.04	0.06	0.08	0.05	0.06	0.06	0.06	0.07	0.05
(22) AATCATCATCGAATGGAATCGAATGG	0.21	0.26	0.36	0.2	0.26	0.18	0.2	0.25	0.22
Cumulative density of abundant repeats	5.64	5.94	8.37	5.58	7.55	4.53	5.03	6.80	5.18
Cumulative density of all repeats	8.94	9.62	13.30	9.31	11.93	7.71	8.47	10.99	8.77

B

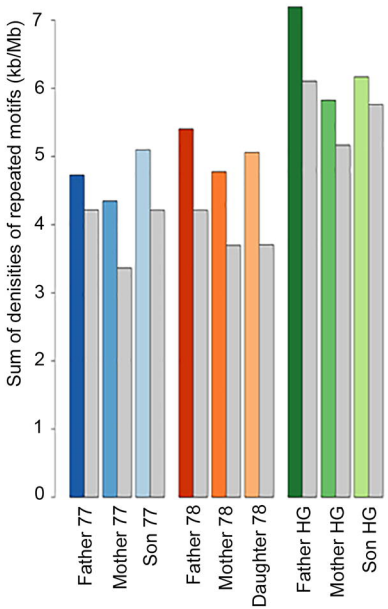

C

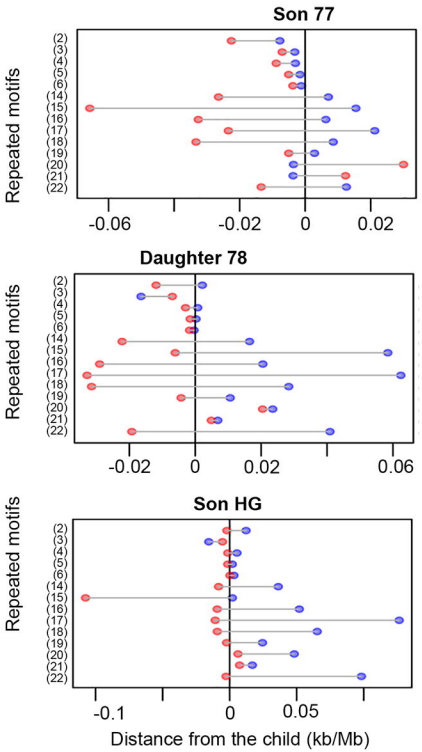

Figure 6

	NANOPORE						PACBIO			
	Gorilla (N=1)	Chimpanzee (N=1)	Bonobo (N=1)	Human (N=1)	S. orangutan (N=1)	B. orangutan (N=1)	Gorilla (N=1)	Chimpanzee (N=1)	Human (N=1)	S. orangutan (N=1)
(1) AATGG	6.92	0.35	4.67	2.93	0.72	1.03	1.97	0.23	0.4	0.36
(2) ACTCC			<0.01				<0.01	<0.01	<0.01	0.02
(3) AAAG	0.08	0.07	0.08	0.1	0.1	0.09	0.01	0.01	0.05	0.05
(4) AATGGAGTGG	<0.01		<0.01	<0.01	<0.01	<0.01	0.01	<0.01	<0.01	0.03
(5) AATGGAATGGAGTGG	<0.01		<0.01	<0.01	0.01	0.02	0.01	<0.01	<0.01	0.03
(6) AATGGAGTGGAGTGG	<0.01					<0.01	<0.01	<0.01	<0.01	0.02
(7) AAGTGGAATGG		<0.01	<0.01	<0.01	<0.01	<0.01	<0.01	<0.01	<0.01	0.09
(8) AATGGAATGTG				<0.01	<0.01		<0.01	<0.01	<0.01	0.04
(9) AAAGTGGAATGG	<0.01			<0.01	<0.01	<0.01	<0.01			0.06
(10) AACGTGGAATGG					<0.01	<0.01	<0.01			0.05
(11) AATGGAATGTGG	<0.01		<0.01	<0.01	0.04	0.05	<0.01	<0.01	<0.01	0.85
(12) AATGGAATGGAATGTGG	<0.01		<0.01	<0.01	0.01	0.01	0.01	<0.01	<0.01	0.09
(13) AATGGAATGGAATGGAATGTGG	<0.01		<0.01	<0.01	0.02	0.02	0.01	<0.01	<0.01	0.33
(14) AAATGGACTCGAATGGAATCATC	<0.01						<0.01	<0.01	<0.01	
(15) AATCGAATGGAATGG			<0.01	<0.01			0.01	<0.01	0.01	<0.01
(16) AAATGGAATCGAATGGAATCATC	<0.01		<0.01	0.01			<0.01	<0.01	0.01	
(17) AATCATCGAATGGAATCGAATGG	<0.01		<0.01	0.11			<0.01	<0.01	0.06	
(18) AATCATCGAATGGACTCGAATGG	<0.01		<0.01	<0.01					0.01	
(19) AATCATCATGAATGGAATCGAATGG	<0.01	0.01	<0.01	0.04			<0.01	<0.01	0.01	
(20) AAATGGAATCGAATGGAATCATCATC	0.01	0.02	<0.01	0.21			<0.01	<0.01	0.05	
(21) AAATGGAATCGAATGTAATCATCATC										
(22) AATCATCATCGAATGGAATCGAATGG	0.05	0.03	0.04	1.15			<0.01	<0.01	0.17	
(23) AAACATGTAAATATTTACACAGAATCTGTAT	0.02	0.39	1.92					0.24		
(24) AAATATCTACACCGCTATCTGTATGAACATGG	19.25	<0.01	<0.01			0.11	4.9	<0.01		
(25) AAATATCTACACCGCCATCTGTATGAACATGG	2.02		<0.01			<0.01	0.5	<0.01		
(26) AAACATGGAAATATCTACACAGCCATCTGTAT	0.03	0.53	0.48			<0.01	<0.01	0.07		
(27) AAACATGGAAATATCTACACCACCATCTGTAT	0.04	0.08	0.1			<0.01	<0.01	0.01		
(28) AAACATGGAAATATCTACACCACTATCTGTAT	0.05	0.04	0.08			<0.01	0.01	0.01		
(29) AAACATGGAAATATCTACACCGCCATCTGTAT	1.67	1.53	2.58		0.01	<0.01	0.43	0.36		
(30) AAACATGGAAATATCTACACCGCTATCTGTAT	3.41	2.06	4.62		<0.01	0.02	2.58	1.01		
(31) AAACATGGAAATATCTACACCGCTATCTGTGT	0.11	0.03	0.13			<0.01	0.16	0.02		
(32) AAACATGGAAATATCTACACTGCCATCTGTAT	0.04	0.23	0.28			<0.01	0.01	0.03		
(33) AAACATGGAAATATCTACACTGCTATCTGTAT	0.12	0.06	0.09				0.01	0.01		
(34) AAACATGGAAATATCTACACCGCGATCTGTAT	<0.01	0.04	0.02				<0.01	0.02		
(35) AAACATGGAAATATCTACACCGCCATCTCTAT	0.29	0.25	0.24			<0.01	0.07	0.04		
(36) AAACATGGAAATATCTACACCGCTATCTCTAT	0.47	0.24	0.33			<0.01	0.12	0.11		
(37) AAATATCTACACAGCTATCTGTATGAACATGG	0.21		<0.01				0.02			
(38) AAATATCTACACCACTATCTGTATGAACATGG	0.03		<0.01				0.01			
(39) AAATATCTACACCGCTATCTGCATGAACATGG	0.05						0.01			
Cumulative density of abundant repeats	34.88	5.96	15.65	4.56	0.90	1.38	10.88	2.17	0.80	2.02

Figure 7

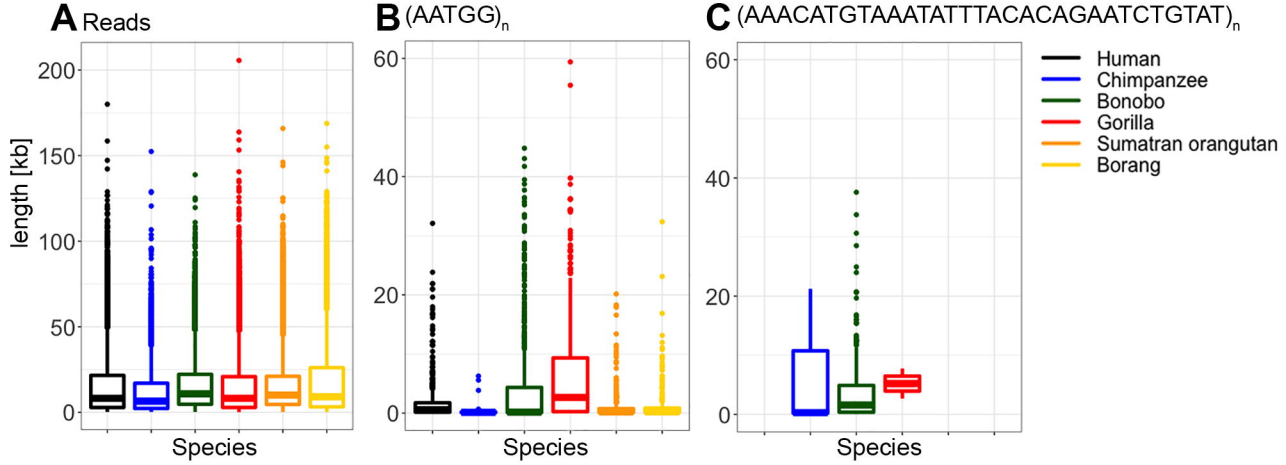
A Reads
B (AATGG)n
C (AAACATGTAAATATTTACACAGAATCTGTAT)n
length [kb]
200
150
100
50
0
60
40
20
0
Species
Human
Chimpanzee
Bonobo
Gorilla
Sumatran orangutan
Borang